



NTNU – Trondheim
Norwegian University of
Science and Technology

The response of a round jet to transverse forcing

Maria Theresia Måløy

Master of Production and Quality Engineering

Submission date: June 2015

Supervisor: James Dawson, EPT

Norwegian University of Science and Technology
Department of Energy and Process Engineering

EPT-M-2014-26

MASTER THESIS

Name: Maria Måløy

Spring 2015

*The response of a round jet to transverse forcing.***Background and objective**

Understanding the formation of coherent vortex structures in turbulent jets has widespread importance in engineering and science. They produce noise, cause flow-structure interaction, and play a key role in exciting thermo-acoustic instabilities in combustion systems from rocket engines to gas turbine combustors. New low-emission aeroengines in stationary gas turbines for power generation and aeroengines suffer from thermosacoustic instabilities which are difficult to predict and therefore cannot ensure a given design will not be unstable. This project focuses on the formation of vortex structures due to interaction with transverse acoustic waves in a single jet and in multiple jets to azimuthal waves in an annulus.

The student will perform the following tasks:

- Conduct pressure and velocity measurements of a round jet subjected to transverse acoustic forcing at different locations along the mode shape.
- Investigate the effect of phase change on the jet response that occurs at the pressure node
- Analyse and compare the data with the existing literature.

Within 14 days of receiving the written text on the master thesis, the candidate shall submit a research plan for his project to the department.

When the thesis is evaluated, emphasis is put on processing of the results, and that they are presented in tabular and/or graphic form in a clear manner, and that they are analyzed carefully.

The thesis should be formulated as a research report with summary both in English and Norwegian, conclusion, literature references, table of contents etc. During the preparation of the text, the candidate should make an effort to produce a well-structured and easily readable report. In order to ease the evaluation of the thesis, it is important that the cross-references are correct. In the making of the report, strong emphasis should be placed on both a thorough discussion of the results and an orderly presentation.

The candidate is requested to initiate and keep close contact with his/her academic supervisor(s) throughout the working period. The candidate must follow the rules and regulations of NTNU as well as passive directions given by the Department of Energy and Process Engineering.

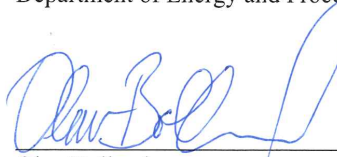
Risk assessment of the candidate's work shall be carried out according to the department's procedures. The risk assessment must be documented and included as part of the final report. Events related to the candidate's work adversely affecting the health, safety or security, must be documented and included as part of the final report. If the documentation on risk assessment represents a large number of pages, the full version is to be submitted electronically to the supervisor and an excerpt is included in the report.

Pursuant to "Regulations concerning the supplementary provisions to the technology study program/Master of Science" at NTNU §20, the Department reserves the permission to utilize all the results and data for teaching and research purposes as well as in future publications.


The final report is to be submitted digitally in DAIM. An executive summary of the thesis including title, student's name, supervisor's name, year, department name, and NTNU's logo and name, shall be submitted to the department as a separate pdf file. Based on an agreement with the supervisor, the final report and other material and documents may be given to the supervisor in digital format.

- Work to be done in lab (Water power lab, Fluids engineering lab, Thermal engineering lab)
 Field work

Department of Energy and Process Engineering, 14. January 2015



Olav Bolland
Department Head



James Dawson
Academic Supervisor

Research Advisor:

Abstract

This project was done in two parts. The first part was to investigate the behaviour of a small jet placed in five different positions between the antinode and the node in an acoustic field. This jet was measured with a hotwire at the jet exit and two microphones inside the jet. The velocity amplitudes from the hotwire and the pressure amplitudes from the microphones were plotted against each other for all five positions. This showed that the size of the pressure amplitudes inside the jet was linear to the velocity amplitudes at the exit, and that the gradient was the same for all positions. The strongest amplitudes were at the antinode and the weakest at the node. The different amplitudes for the five positions were compared to the theory of an acoustic field inside a box, and compared well, indicating that the measurements were done correctly.

The second part was a larger jet that was acoustically forced with the node placed at the centre of the jet. Eight microphones were mounted flush around the jet with 45° between them, right beneath the jet exit. The pressure inside the jet was measured with these eight microphones for two different resonance frequencies. This was done to see how the steepness of the gradient affected the measurements. The results from the highest resonance frequency compared well with theory, but the results from the lower did not. All the signals from the lowest resonance frequency had a phase shift. This was investigated, and it concluded with that the amplitudes from the speakers were different.

Sammendrag

Denne masteroppgaven er todelt. Den første delen undersøker oppførselen til en liten jet som er plassert i fem forskjellige posisjoner mellom en antinode og en node i et akustisk felt. Jeten ble målt med en hotwire ved utgangen og med to mikrofoner inne i jeten. Hastighets-amplitudene fra hotwireren og trykk-amplitudene fra mikrofonene ble plottet mot hverandre for alle fem posisjonene. Denne grafen viste at trykk amplitudene inne i jeten var lineær i forhold til hastighets amplitudene ved utgangen. Den viste også at stigningstallet var det samme for alle fem posisjonene. De sterkeste amplitudene var ved antinoden og de svakeste ved noden. De forskjellige amplitudene for de fem posisjonene ble sammenlignet med teorien til et akustisk felt inne i en boks og dette stemte godt overens. Dette indikerte at målingene ble gjort riktig.

Den andre delen bestod av en større jet som ble påvirket av et akustisk felt der noden ble plassert i midten av jeten. Åtte mikrofoner ble plassert i en sirkel parallelt med jet veggen rundt røret med 45° mellom seg. De ble plassert rett under utgangen til jeten. Trykket inne i jeten ble målt med de åtte mikrofonene for to resonans frekvenser for å se hvordan helningen på stigningstallet påvirket målingene. Resultatene fra den høyeste resonans frekvensen stemte godt overens med teorien, mens resultatene fra den lavere resonansfrekvensen ikke gjorde det. Alle signalene fra den lavere resonans frekvensen hadde en faseforskyvning. Dette ble undersøkt, og konkludert med at amplitudene fra høytalerne var forskjellige.

Preface

This master thesis is written for the Department of Energy and Process Engineering (EPT), at the Norwegian University of Science and Technology (NTNU) during the spring of 2015.

I would like to thank my supervisor James Dawson for all the help he has given me and the guidance through out this school year. I would also like to thank Arnt Egil Kolstad and Øyvind Hanssen-Bauer for their help in the lab.

And thanks to my mother who has always been there for me...

Trondheim 2015

Maria Theresia Hasund Måløy

Contents

Abstract	iii
Sammendrag	v
Acknowledgements	vii
Contents	ix
1 Introduction	1
1.1 Motivation	1
1.2 Previous studies	2
1.3 The master thesis structure	3
2 Experimental setup	5
2.1 Apparatus 1: The small jet	6
2.2 Apparatus 2: Big jet	8
2.3 Instrumentation and Measurement	11
2.3.1 Speakers	11
2.3.2 Mass Flow Rates	11
2.3.3 Hotwire measurements	12
2.3.4 Microphones	12
3 Theory	15
3.1 Standing modes	15
3.2 Hot-wire measurements	18
3.2.1 Temperature correction	20
3.2.2 Least squares method	21
3.2.3 Square wave test	23
3.3 Fourier	24
3.3.1 Phase shift	25
3.3.2 Matlab	26

3.4	Nyquist theorem and quantization	27
3.4.1	Sampling values in the experiments	29
3.5	Turbulent vs laminar velocity profile	30
4	Preparations for the small jet	31
4.1	Calibration of hotwire	31
4.2	Temperature correction	32
4.3	Square wave test	32
4.4	Jet profiles	34
4.5	Calibration of microphones	35
4.6	Frequencies	36
5	Forcing of the small jet	39
5.1	The positions of the jet	39
5.2	The velocity amplitudes	40
5.3	The pressure amplitudes	43
5.4	The Positions compared to each other	44
5.5	Comparing results with theory	48
6	Forcing of the big jet	51
6.1	Low forcing frequency	52
6.1.1	Why not as predicted	55
6.1.2	With airflow	57
6.2	High forcing frequency	59
6.2.1	With airflow	64
7	Conclusion and future work	67
7.1	Experimental uncertainties	67
7.1.1	Measurements	67
7.1.2	Accuracy of the signals	68
7.2	Conclusion	69
7.3	Recommendations for further work	70
	Bibliography	71
	A	75
	B	77
	C	79
	D	81
	E	83

List of Figures

87

List of Tables

89

Acronyms and abbreviations

CT Constant Temperature

HW Hot wire

SLPM Standard Litres Per Minute

DFT Discrete Fourier Transform

OpAmp Operational Amplifier

FFT Fast Fourier transform

cDAQ compact Data Acquisition

Nomenclature

α	The temperature coefficients of the hot wire
Δf	Frequency “bins ”
\hat{f}_n	Frequency spectrum
λ	Number of modes
ν	Kinematic viscosity
τ_w	Time response for a hotwire
A	Gain
A_m	Amplitude range
c	The speed of sound
c_n	Amplitude
E	The measured voltage
E_{off}	The voltage offset
$E_{w,r}$	The wires reference voltage
E_w	Temperature corrected reference voltage
F	Frequency filter
f_c	The upper limiting frequency of a hotwire
F_s	Sampling frequency
h	The height of a square wave peak
L_{box}	The length of the box
Op	The operating settings for the hotwire
Q	Quantization error

q	The sum of the distance from the points to the line squared
R	Samples per seconds needed to measure a frequency adequately
R_b	Two equally sized bridge resistance
R_a	The resistance in the cable plus the hotwire at 300 °C
R_{Cable}	The resistance in the cable
R_{HWcold}	The resistance in the hotwire at 20 °C
R_{HWhot}	The resistance in the hotwire at 300 °C
$R_{tot,5m}$	The measured hotwire resistance at 20 °C with a 5 meter cable
Re	Reynolds number
T_a	The measured temperature at the jet exit
T_c	Constant equal to 20 °C
T_w	Constant equal to 300 °C
x_j	The distance from the y axis in the x direction for each point
x_k	Sample values
y_j	The distance from the x axis in the y direction for each point
e	The bridge unbalance in a hotwire
M1-M12	Microphone positions in the big jet
N	Number of measured points
n	Number of bits
P1-P4	Microphone positions in the small jet

Chapter 1

Introduction

Reducing emission gasses and increasing the efficiency in turbines, is currently a driving force for developing new technology for modern gas turbines. A problem with developing this new technology is instabilities in the combustion chamber. These thermo acoustic instabilities initially explained by Rayleigh can lead to high-cycle fatigue, reduce operability, and increase emission. [34] [25] Thermo acoustic instabilities occurs when the interaction between flames, synchronize with acoustic waves. This creates pressure oscillations which amplitude results in mechanical vibrations that cause severe damage to the engine [18] [29]. Gas turbines have to be operated away from set points where these instabilities occur, limiting their operation range.

1.1 Motivation

This master thesis focus on an acoustically forced jet and how the formation of vortex structures behave in a turbulent jet. This has a widespread importance since they produce noise, causes interaction between flow structures and is an important factor in thermo acoustic instabilities. Low emission aero-engines, jet engines and gas turbines all suffer from thermo acoustic instabilities and it is therefore important to learn more about it to be able to ensure that a given design will not be unstable. By learning more about the formation of coherent vortex structures a small step in the right direction is achieved.

1.2 Previous studies

Even though there have been much progress in this field it is still not possible to theoretically or numerically predict the thermo acoustic stability limits accurate [32]. A lot of work has been done to learn more about the thermo acoustic couplings. Many have acoustically forced a turbulent or a laminar V-flame to learn more about the interaction between the flames and the pressure changes from the sounds. [23] [22] [33] [26] [27] [35] Most of the articles investigates the response with flames, but have done the test on the same settings without flames to have something to compare with. The most interesting articles will be mentioned here.

Lespinnasse et al. [23] is worth mentioning, since parts of this article have similarities with this master thesis. They have placed a V-flame at different positioned of an acoustic transverse field. They have investigated the interaction between the V-flame and the acoustic field, finding the limit for where the oscillation for the flame begins and where there is a flame blowout for the different positions. Other interesting investigations they have done are the shapes of the flames from the pressure antinode to the node and the median curves of the flames. Short summarized: they have looked at the flame and jet dynamics at the pressure antinode and the asymmetrical response at the other positions. They concluded that pressure measurements are not enough to determine the thermo-acoustic coupling, and that acoustic velocity combined with the pressure gradient needs to be investigated to understand the response of the system.

Another interesting article comes from Baillot and Lespinasse [22]. They have investigated the interaction between the acoustic transverse wave and a V-burner at the pressure antinode. Which can change the vertical flow and in some cases make the flow reversed, "plugging". This mechanism generates vortical structures which they have investigated in detail. They have looked on the visible response of the flame, the mechanism that drives the perturbed flow, and the structure of the perturbed jet.

O'Connor and Lieuwen [33] have acoustically forced a burner in the transverse direction, and O'Connor et.al. [26] have acoustically forced an annular jet in the transverse direction. Both papers have investigated the characteristics of the burner and analysed the multidimensional disturbance field caused by the acoustic. They found out that the flow field near the nozzle works as superposition of acoustic and vortical disturbances, and that different disturbances affect different portions of the flow. An interesting observation done by both papers is that the right and left side of the burner oscillates out of phase with each other when the pressure node is at the centre, and that the burner responds symmetrically around the burner when the pressure antinode is at the centre. This has some similarities to the second part of this master thesis.

Considering all the studies that have been done on a single axisymmetric flame subjected to acoustic forcing, only recently experiments in simplified annular combustion chambers have been started to expose the complex physical mechanism that drives the instabilities in an annular combustion chamber. [38] [28] [20] [19] [37] these studies take it a step further than what have been done in this thesis.

1.3 The master thesis structure

This master thesis is divided into six chapters with two experiments. The first experiment was on a small jet placed in five different positions between the antinode and the node. The second was an experiment on a big jet where the node was placed at the centre of the jet. The first chapter explain the experimental setup for both and give an overview of the equipment that is used. The next chapter describes the theory that is needed to understand the experiments and the underlying concepts. The experiments are divided into three chapters, the first chapter considers the preparations for the experiment for the small jet, and the second chapter present the results for the small jet. The third is the results for the big jet. Finally, the conclusions are drawn and future work is considered in the last chapter.

Chapter 2

Experimental setup

This chapter describes the two different setups that have been used during the experiments. The first setup is for a small jet, while the second setup is for a larger jet. Both are placed inside the same dimensional box and are forced with two speakers. Both setups use microphones to measure the pressure at different places inside the jet and box. The small jet also uses a hotwire to measure the velocity at the exit. At the end of this chapter the equipment that has been used in both experiments are described, and the specifications of the instrumentation.

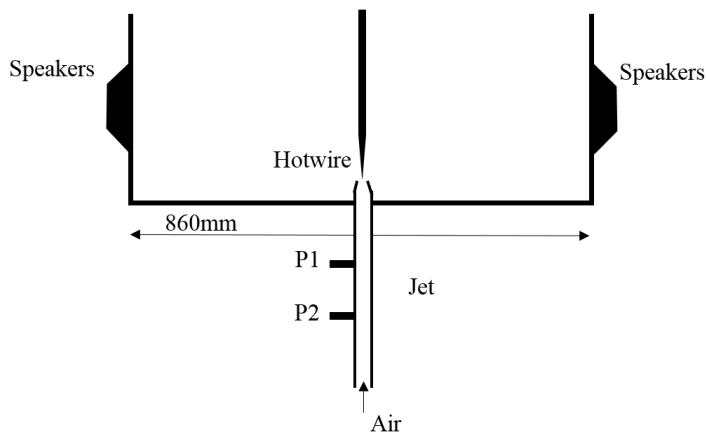


Figure 2.1: Schematics of the small jet and the box, the long side view 860 mm

2.1 Apparatus 1: The small jet

Figure 2.1 shows the schematic of an acoustically forced small jet. It displays the box from the long side 860 mm, with the hotwire at the tip of the jet, and the speakers at the side walls. The box has dimensions 860 mm, 150 mm and 400 mm. The speakers were mounted on the walls 70 mm from the bottom. Microphone 1 and 2 (P1 & P2) are placed at the side of the jet. Figure 2.3 shows a picture of the setup with a picture of the placement of the hotwire in Figure 2.4.

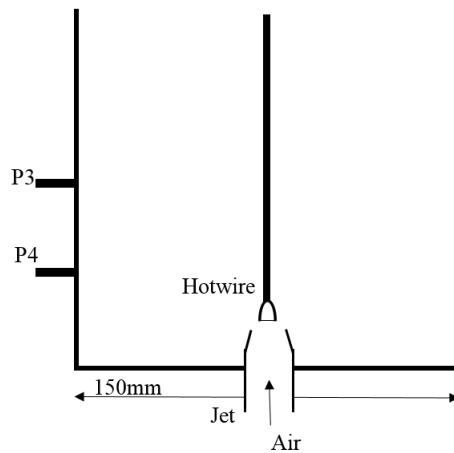


Figure 2.2: Schematics of the box, side view 150 mm

The short side view of the box and the hotwire is displayed in Figure 2.2. The figure displays the microphones P3 and P4 and their placement. The microphones were placed 75 mm and 110 mm above the bottom at the same position as the jet. The speaker walls were movable and therefore the microphones (P3 & P4) were always placed at the same position as the jet. Moveable walls made it possible to place the jet at any position in the pressure sound field inside the box.

The tip of the jet extended 25 mm above the bottom of the box, as can be seen from Figure 2.4 and Figure 2.2. The diameter at the exit is 10 mm, and the diameter in the main pipe is 34 mm. The tip is 65 mm high, and the distance from the top to P1 is 165 mm and 365 mm to P2. See Figure 2.5

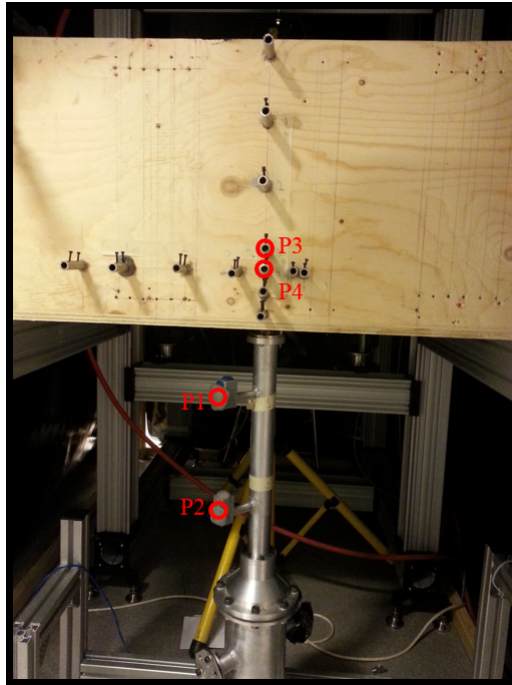


Figure 2.3: Picture of the setup for the small jet



Figure 2.4: Picture of the hotwire above the jet, seen from the 860 mm side view

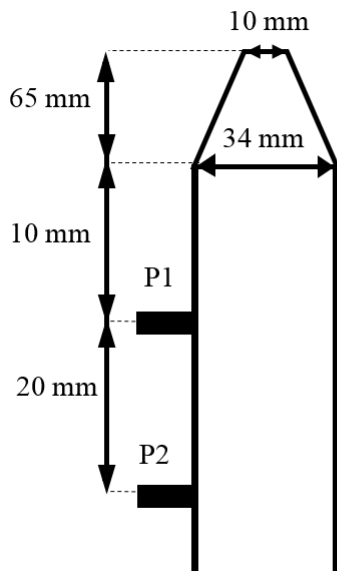


Figure 2.5: The dimensions of the small jet

2.2 Apparatus 2: Big jet

The second setup was for a big jet: This was placed inside the same box but the exit of this jet was at the same level as the bottom of the box. The big jet had an inner diameter of 75 mm and a circular disc with 8 microphones (M1-M8) placed around the jet 22 mm below the exit, see Figure 2.6 and Figure 2.7. The length of the jet was 800 mm plus a cone at the bottom. This cone had an expansion angle of $\beta = 20^\circ$. At the bottom of the cone there was a 30 mm long cylinder with an inner diameter of 8 mm that was used to connect the jet with the air hose.

The 8 microphones were mounted flush to the jet wall and were equally spaced around the jet with an angle of 45° , see the picture in Figure 2.7. Microphone 3 and 7 were parallel to the 860 mm wall while Microphone 1 and 5 were parallel to the speaker walls, see Figure 2.8.

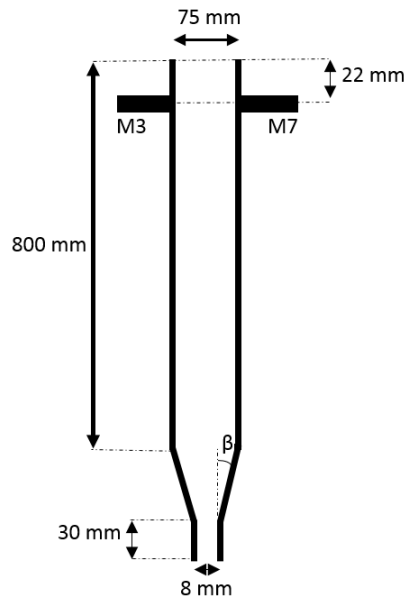


Figure 2.6: The dimensions of the big jet



Figure 2.7: Picture of the setup of the microphones around the big jet

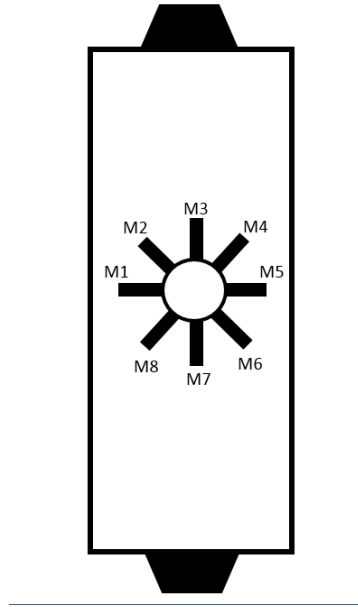


Figure 2.8: The placement of the microphones seen from the top view

Four extra microphones were placed on the wall (M9-M12). These microphones were placed 74 mm above the bottom of the box and 308 mm, 386 mm, 430 mm and 472 mm from the speaker wall for M9, M10, M11 and M12. See Figure 2.9. This made Microphone 11 placed at the very centre of the jet.

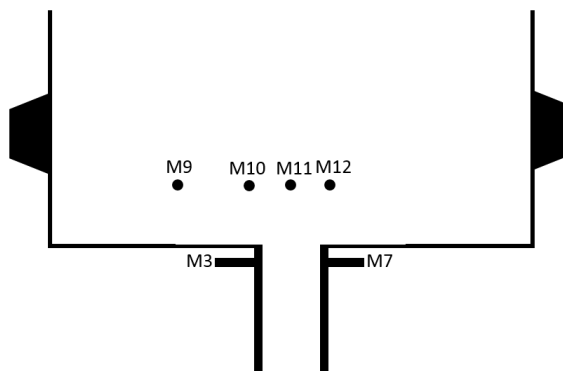


Figure 2.9: The placement of the microphones on the wall

2.3 Instrumentation and Measurement

The equipment used in the two experiments were the same. The same speakers, microphones, box and mass flow controller was used by both. The only exception was the hotwire, which was only used in the first setup by the small jet.

2.3.1 Speakers

A Wavetek 4MHz Function generator was used to generate a sine signal that was amplified by a Crown CE 1000A amplifier and sent to the speakers by a split cable. The speakers was of the type Rondson TU-100 and had a range between 150 Hz and 10 000 Hz according to @rtech a firm that sells them [8], but experience at the lab shows that the limit is closer to 250 Hz. Figure 2.10 shows the speakers and the setup for the speakers used during the experiments.

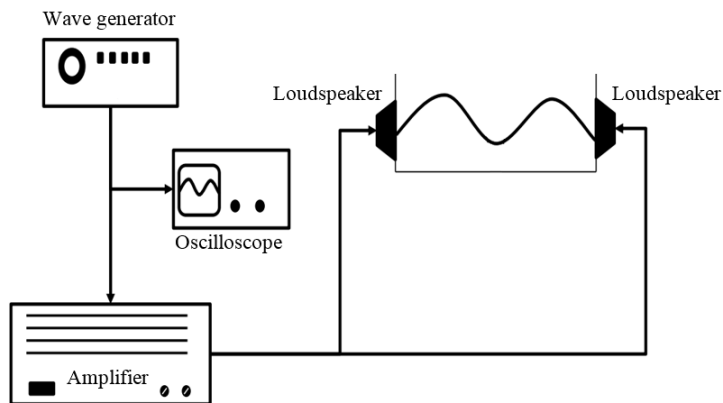


Figure 2.10: The setup for the box with the wave generator, oscilloscope, amplifier and the speakers [17]

2.3.2 Mass Flow Rates

The air flow to the jet was controlled by a mass flow controller. The flow rates Standard Litres Per Minute (SLPM) were used to calculate the average velocity U at the jet exit. The velocity used in the experiments were between 0.5 m s^{-1} and 40 m s^{-1} , and how the velocities were calculated and the more accurate velocities can be seen in Appendix A

2.3.3 Hotwire measurements

There were used several hotwires during the experiments on the small jet and the resistance were between 6.5Ω and 6.7Ω . When the hotwires were used they was placed at the centre of the jet, parallel to the speaker walls. This made the hotwires able to measure the sound waves propagating back and forth between the speakers. (If placed perpendicular to the speakers the sound waves would not affect the hotwire, and if it was placed obliquely the sound waves would hit the wire uneven.) To measure these sound waves samples were taken with 20 000 Hz for four seconds, then they were digitalized by a compact Data Acquisition (cDAQ) 16 bit resolution with a ± 10 V range.

The range for the hotwires were 1-2 V when not amplified. The signals were therefore amplified as much as possible while still inside the ± 10 V range. All the hotwires were amplified with a gain equal to 8.

The wire used in the hotwires were Wollaston $5 \mu\text{m}$ wire and had a sensitivity of $\alpha=1.69 * 10^{-3} \Omega/^{\circ}\text{C}$

The tip of the hotwires or the wire were 2-3 mm and the length of the hotwires were approximately 10 cm long.

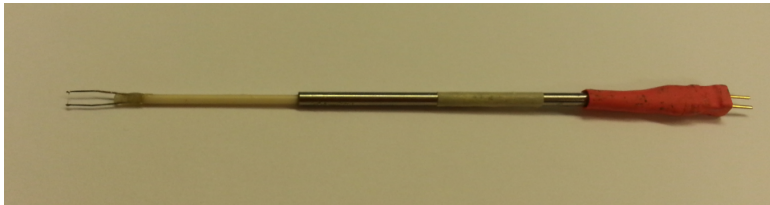


Figure 2.11: Picture of one of the hotwires used.

2.3.4 Microphones

Four different placements for the microphones were used in the first setup P1-P4, and twelve different placements were used for the second M1-M12. Figure 2.12 shows the setup for the microphones used during the experiments.

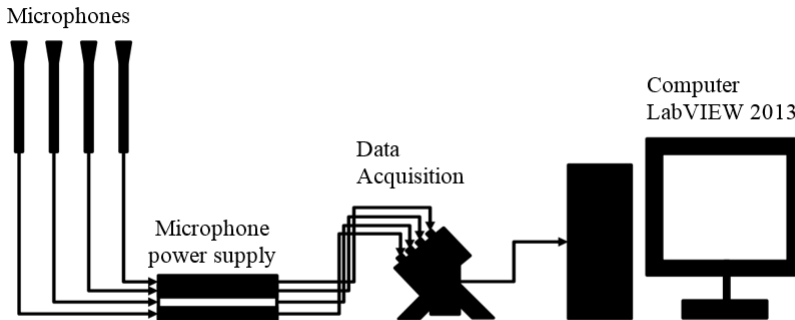


Figure 2.12: The setup for the microphones [17]

Table 2.1 shows the sensitivity of all the microphones. Microphone P4, was used as the reference when changing the measured volt back to pressure for the first setup. Microphone M1 was used for M1-M8 and M10 was used as the reference for M9-M12 in the second setup.

Microphone	Sensitivity		
M1/P1	4,27	mV/Pa	
M2/P2	4,13	mV/Pa	
M3/P3	4,07	mV/Pa	
M4/P4	4,14	mV/Pa	
M5	4,13	mV/Pa	
M6	4,14	mV/Pa	
M7	4,31	mV/Pa	
M8	4,08	mV/Pa	
M9	(old)	1,665	mV/Pa
M10	(old)	1,505	mV/Pa
M11	(old)	1,597	mV/Pa
M12	(old)	1,465	mV/Pa

Table 2.1: Table of the sensitivities of the different microphones.

All the microphones had a range from 4 - 100 000 Hz [1], were the samples were taken with 51 200 Hz for two seconds and were digitalized with a cDAQ 24 bit

resolution and ± 5 V range.



Figure 2.13: Picture of a microphone used in the experiments [1]

Chapter 3

Theory

This chapter contains relevant theory that is used during both experiments or in the preparations of the experiments. First it describes standing modes which is the theory behind the sound waves propagating back and fourth inside the box. Next there is a big section on hotwires. This section is particularly for the small jet. It describes the general theory of the hotwire in the beginning and then there are three sub sections about the use of a hotwire. The first sub section describes how to compensate for temperature changes in the air. The second is the theory for finding a curve that fits the measured calibration points, and the third is the theory to find the velocity fluctuation limit. After the hotwire theory there is a section about Fourier. Fourier is relevant for both experiments since finding the amplitude and the frequencies of the measured signals are relevant in both cases. There is also a small section about finding the phase shift for a sine signal. Then there is a section about sampling the measurements and how the signals get digitalized. The last section is a short section about velocity profiles in a pipe. This was relevant for the small jet since the velocity profile gets measured by a hotwire.

3.1 Standing modes

Sound can be viewed as a wave motion in air that changes the pressure in the air as it propagates forward. These pressure changes are measured and used when searching for instabilities. Instabilities occur when energy is absorbed from the sound and makes the box vibrate at a resonance frequency [21]. To be able to find these resonance frequencies or eigenfrequencies, some basic understanding of waves is needed. “Standing waves occur when two waves with the same amplitude and

frequency, travel in the opposite direction, interact. "also called wave interference, see figure 3.1 [36, p. 451-452]

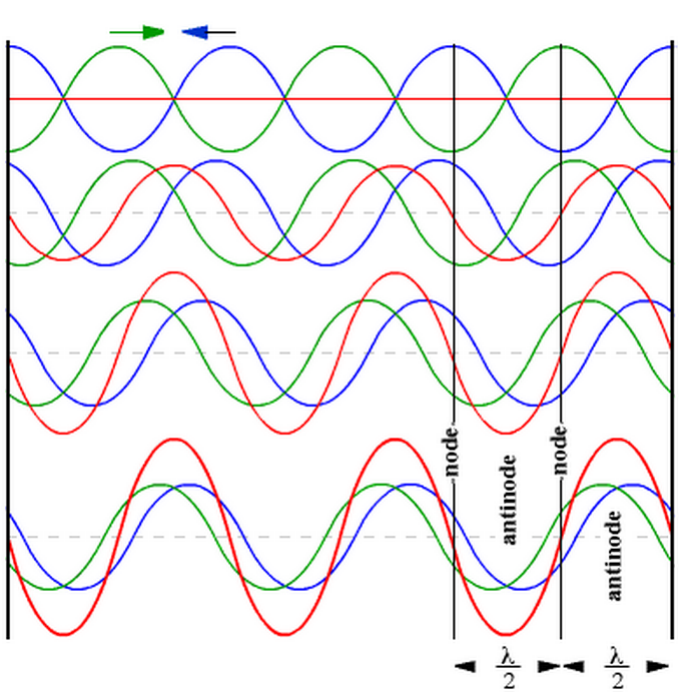


Figure 3.1: The interaction between two waves from opposite direction, equal frequency and magnitude reinforcing each other. See the red line [12]

A standing wave has fixed nodes in space where the two waves cancel each other out and fixed antinodes in space where they reinforce each other, see Figure 3.1. The number of nodes and antinodes depends on the modes

$$\lambda_1, \lambda_2, \lambda_3, \lambda_4, \dots$$

excited. For a one dimensional case the resonance frequencies of a box can be calculated by

$$f = \frac{c\lambda}{2L_{box}} \quad (3.1)$$

Where f is the frequency, λ the number of modes, c the speed of sound and L_{box} is the length of the box.

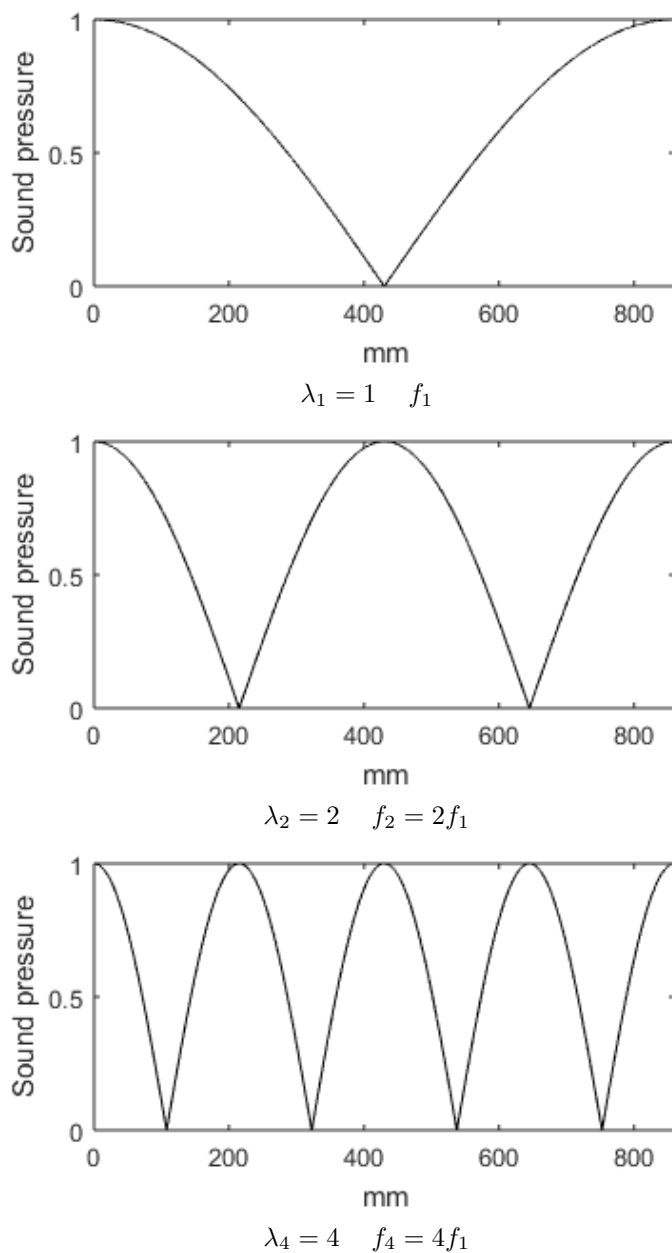


Figure 3.2: Resonance frequencies of pressure modes in a one dimensional box, 860 mm

For a box with closed walls this means that the antinodes, will be at the walls, as seen in Figure 3.2. The number of fluctuations in the box depend on the mode excited, λ .

For the one dimensional equation to be valid the aspect ratio of the box has to be right. The length has to be much bigger than the width or the height, making the frequency of the signal in the length direction too low to propagate f_1 the other directions. Meaning that the length of the box needs to be much bigger than the height and width to avoid two or three dimensional effects [21]

3.2 Hot-wire measurements

Hot-wire is a research tool in fluid mechanics, that measures the velocity in a fluid and makes it possible to study the detailed fluctuations in a turbulent flow. In this experiment a Constant Temperature (CT) anemometer is used. It consist of a small electrical Hot wire (HW) that is exposed to air, and electrical equipment that is connected to it, see Figure 3.3. The operating principle is simple: the wire is cooled as it loses heat to the surrounding flowing air, where the electrical system provides the hot wire with the right amount of voltage so it can maintain a constant temperature. The higher the flow velocity, the higher rate of heat from the sensor and thus a higher voltage across the hotwire. [16, p. 393]

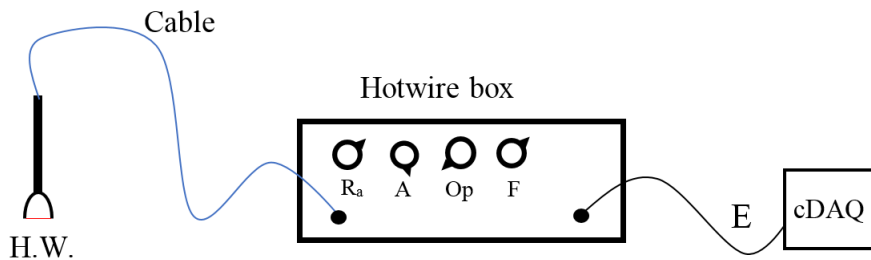


Figure 3.3: Hot-wire box connected to hotwire and cDAQ

A simple figure of the hotwire and the equipment connected to it is displayed in Figure 3.3, with the most important settings marked inside the hotwire box in the figure. The cable and the hotwire is marked with blue and red respectively and are the only equipment in the control circuit that is outside the hotwire box. R_a is the hotwire resistance that is calculated and used when operating the hotwire. Described in more detail later in this section. A is the gain and amplifies the measured signal E before it is sent to the cDAQ where the signal is digitalized. It is important that the signal is amplified as much as possible but still within the cDAQs range. The cDAQ had a range of 20 V, meaning that the difference between the highest measured volt at 40 ma^{-1} and the lowest 0 ms^{-1} could not exceed 20 V. O_p , the operating setting had three different operations, stand by, operating and square wave. Where the operating mode was used during experiments, the stand by when handling the hotwire or moving it and the square wave when finding the limiting frequency. The filter F , filtered away frequencies above a chosen frequency.

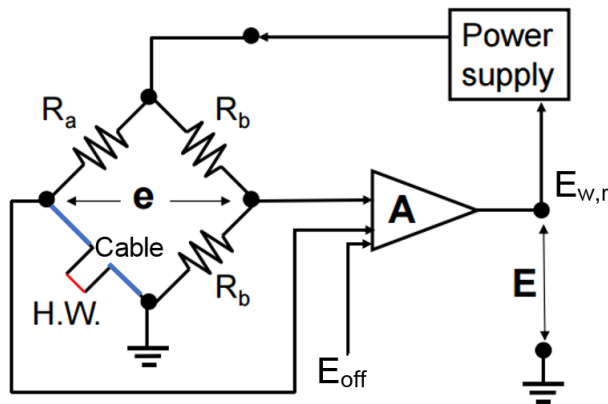


Figure 3.4: Hotwire CT control circuit [15, p. 27]

Figure 3.4 displays the simplified control circuit of the hotwire. Where the red line represent the wire in the hotwire and the blue line the cable, corresponding to the colours in Figure 3.3. R_a is the resistance equal to the cable plus the hotwire at $300 \text{ }^\circ\text{C}$, and needs to be calculated [15, p. 27]. R_b is two equally sized bridge resistance making the bridge unbalance e a way to measure if the hotwire is $300 \text{ }^\circ\text{C}$. e should ideally be 0, if not the voltage needs to increase or decrease to be able to raise or lower the resistance/heat out of the hotwire. To determine if the value e needs to be changed, the circuit has an Operational Amplifier (OpAmp), marked as A that is used to control damping and adjusts the voltage sent in. The opAmp measures e and in combination with a offset value E_{off} adjusts the voltage sent to the hotwire. E_{off} is known as the input offset value and is used by the

opAmp to make \mathbf{e} zero. Ideally if \mathbf{e} is zero, the op Amp should measure \mathbf{e} as zero. In practice, a small differential voltage must be applied to the input to force the output to zero. This is known as the input offset voltage, E_{off} . [2] [7]

\mathbf{E} is the measured voltage and consist of the adjusted Anemometer output in voltage $E_{w,r}$, and the offset voltage E_{off} that have been amplified. [13, p. 844] [24, p. 205]

$$E = A(E_{w,r} + E_{off}) \quad (3.2)$$

E_{off} can be obtained by setting the gain to 1 and measuring the E_{output} on the hotwire box, and multiply it with the gain.

The unknown resistance R_a can be calculated by:

$$R_a = R_{HW_{hot}} + R_{Cable} \quad (3.3)$$

$$R_{Cable} = R_{tot,5m} - R_{HW_{cold}} \quad (3.4)$$

$R_{tot,5m}$ is the measured hotwire resistance at 20 °C with a 5 meter cable, $R_{HW_{cold}}$ is the measured hotwire resistance at 20 °C. By subtracting $R_{HW_{cold}}$ from $R_{tot,5m}$ the resistance in the cable R_{cable} is obtained, the blue line. The resistance in the hotwire at 300 °C, the red line can be calculated by:

$$R_{HW_{hot}} = R_{HW_{cold}}(1 + \alpha(T_w - T_c)) \quad (3.5)$$

Where α is the temperature coefficients of the hot wire, T_w is the temperature of the heated wire 300 °C, while T_c is the reference temperature of 20 °C. [14][15, p.30].

3.2.1 Temperature correction

Since the hotwire is very sensitive to temperature changes, a small measuring device was placed on the hotwire to measure the temperature of the air exciting the jet. Since there is variation in the resistance with the temperature, the measured volts was corrected compared to the standard temperature 20 °C, from the measured temperature using the original voltage equation 3.2

$$E = A(E_{w,r} + E_{off})$$

E_w can be corrected with the following equation:

$$E_w = E_{w,r} \frac{T_w - T_a}{T_w - T_c} \frac{1}{2} \quad (3.6)$$

Where T_w is the temperature of the heated wire 300 °C, T_a is the measured temperature, T_c is the reference condition 20 °C and $E_{w,r}$ is the reference wire voltage. By setting the new E_w back into the original equation the new and temperature corrected voltage have been obtained. [14, p.47 and p.215]

$$E = A(E_w + E_{off}) \quad (3.7)$$

3.2.2 Least squares method

Least squares method was used when calibrating the microphones and calibrating the hotwire. Matlab functions were used to do these fittings automatically and the theory behind them are described in this section.

For the microphones a least squares method for a straight line was needed, a curve fitting tool called `cftool` from Matlab did this automatically. The hotwires needed a polynomial fit of 4th degree, for this there were a function called `polyfit` in Matlab. The principals for fitting a straight line and a 4th degree polynomial were the same.

For a straight line

$$y = a + bx$$

fits through the given points $(x_1, y_1), \dots, (x_N, y_N)$. “So that the sum of the squares of the distances of those points from the straight line is minimum, where the distance is measured in the vertical direction”[30, p.860].

To be able to find the best line through the given points, see Figure 3.5, it is possible to take sum of the squared distance from x_j to the line:

$$q = \sum_{j=1}^N (y_j - a - bx_j)^2 \quad (3.8)$$

Where N is the number of points, q is the sum of the distance from the points to the line squared, x_j is the distance from the y axis in the in the x direction for each point and y_j is the distance from the x axis in the y direction for each point .

For a polynomial fitting this means:

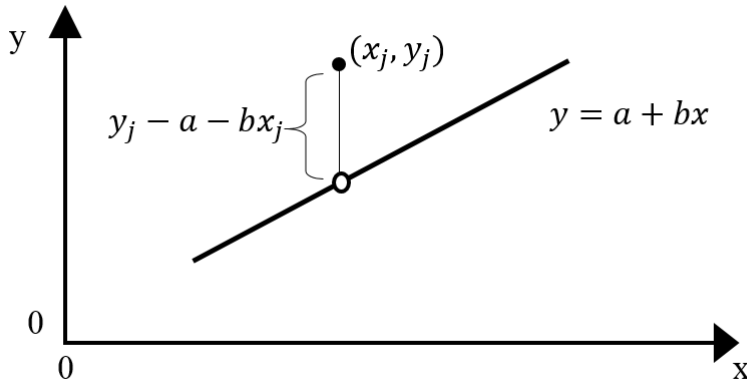


Figure 3.5: Vertical distance of a point (y_j, x_j) from a straight line $y = a + bx$

$$q = \sum_{j=1}^N (y_j - p(x_j))^2 \quad (3.9)$$

where

$$p(x_j) = a + b_1x + \dots + b_Nx^N \quad (3.10)$$

To be able to find the minimum distance both for the linear and the higher order it is needed to find the derivative of q for all the unknowns. For a straight line this means a and b :

$$\frac{\partial q}{\partial a} = 2 \sum (y_j - a - bx_j) = 0 \quad (3.11)$$

$$\frac{\partial q}{\partial b} = 2 \sum x_j (y_j - a - bx_j) = 0 \quad (3.12)$$

This gives two equations with two unknowns.

$$aN + b \sum x_j = \sum y_j \quad (3.13)$$

$$a \sum x_j + b \sum x_j^2 = \sum x_j y_j \quad (3.14)$$

By finding a and b we find the best possible line representing the measured points. For a polynomial of 4^{th} order it is the same procedure to find the unknown numbers, but instead of two equations there will be five equations and five unknown. [30, p.859-862] [9] [10]

A 4^{th} degree polynomial is the recommended degree polynomial for a hotwire calibration according to D. Olivari and M. Carbonaro [24, p.209][15, p. 39]

3.2.3 Square wave test

To determine the limiting frequency of the hotwire a square wave test can be used. A square wave test is a technique to measure the time response of a hotwire, by sending in a square wave. By doing this it is possible to measure the time it uses to stabilize the peak.

Figure 3.6 shows the typical response of a CT hotwire that undergoes a square wave test. As can be seen from the figure the time τ_w is the time from the start of the pulse until the response signal has decayed to be 3 % of the original height, h .

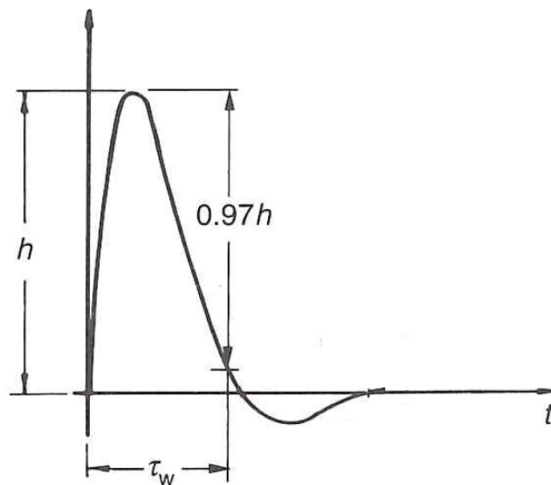


Figure 3.6: The square wave test response of a CT hotwire, the peak [14, p.52]

The measured τ_w can further be used to calculate the upper limiting frequency f_c of the hotwire by:

$$f_c = \frac{1}{1,3\tau_w} \quad (3.15)$$

[14, p.52] [24, p. 206]

3.3 Fourier

A Fourier transform is a good tool to find the amplitude, the power or the frequency of a signal. It can be used to find the strongest frequencies and the combination of frequencies in the signal. In this experiment only the amplitude and the frequency are needed. Figure 3.7 displays what a Fourier transform does to a sine signal. By Fourier transforming a signal, the result becomes a spectrum that displays the amplitude and the frequency of the signal.

If the sine signal in Figure 3.7 had been a combination of several sine signals, the spectrum would have had several peaks. It would display the amplitudes of these signals and the different frequencies.

Discrete Fourier Transform (DFT) is a form of Fourier transform with a finite number of points, where the samples are equally spaced. DFT is the Fourier transform that is used when dealing with samples instead of functions. The samples used in Fourier transformation is normally very large and to minimise the number of operations needed a Fast Fourier transform (FFT) can be used. The FFT is a computational method of the DFT that needs only $o(N) \log_2 N$ operations instead of $O(N^2)$, which make FFT a practical tool for large N. [30, p. 520-525] [5][4]

Kreyszig defines the Fourier transformation to find the frequency spectrum \hat{f}_n of a signal [30, p. 525]:

$$\hat{f}_n = Nc_n = \sum_{k=0}^{N-1} f_k e^{-inx_k} \quad (3.16)$$

Where \hat{f}_n is a complex number that contains the amplitude of a sinusoidal component of function f_k , where N is the number of samples and x_k are the samples.[3] To obtain the amplitude, where the Fourier transformation \hat{f}_n is represented with a fft function in Matlab:

$$c_n = \frac{|\hat{f}_n|}{N} = \frac{|\text{fft}(x_k)|}{N}$$

The frequency “bins” Δf that is plotted against c_n is dependent of the sampling rate and the numbers of points acquired.

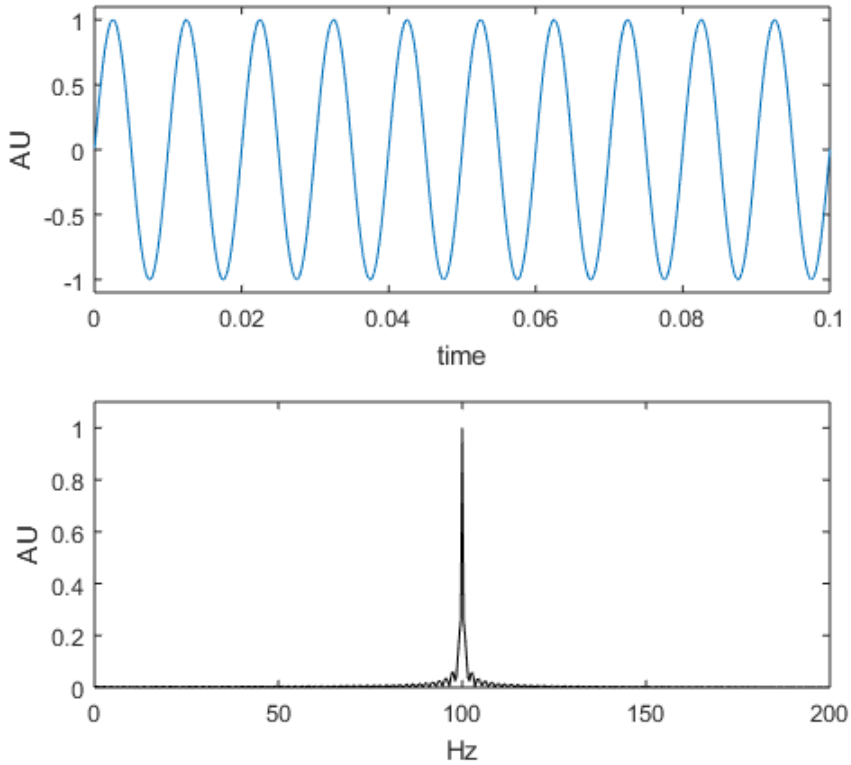


Figure 3.7: Sine signal with amplitude 1 and frequency of 100 hz, Fourier transformed to become an amplitude spectrum

$$\Delta f = \frac{F_s}{o(\log_2(N))} \quad (3.17)$$

Where F_s is the frequency at which the acquired time-domain signal was sampled, and N is the number of samples. $o(\log_2(N))$ is rounded up to the nearest whole number. Meaning for a microphone with 102400 samples the $o(\log_2(102400))=16,64$, but is rounded up to 17, making the frequency bins 0,39 Hz when the sampling frequency is 51200 Hz. [6]

3.3.1 Phase shift

To find the phase shift between two sine signals it is possible to take the arctangent of the imaginary numbers divided on the real numbers from the Fourier transform.

mation for each sine wave. The output from this is in radians and is measured in the counter-clockwise direction. There is a function in Matlab that does this for automatically, called `angle`.

$$\text{Phase}[\text{fft}(x_k)] = \arctangent \frac{\text{imag}[\text{fft}(x_k)]}{\text{real}[\text{fft}(x_k)]} \quad (3.18)$$

$$\text{Phase spectrum in degrees} = \frac{180}{\pi} * \text{Phase}[\text{fft}(x_k)] \quad (3.19)$$

After changing it from radians to degrees, subtract one sine wave from an other to get the phase difference between the signals. Then find the phase difference for the wanted frequency. [6][30, p.607]

3.3.2 Matlab

When Fourier transforming the signal in Matlab, the Fourier transformation \hat{f}_n is represented with a `fft` function in Matlab. `fft` takes in the measured values x_k and the $\log_2(N)$ number and Fourier transforms it, see Figure 3.8. First the values are changed to amplitudes, before it is converted from a two sided spectrum to a one sided spectrum. When converting the spectrum the amplitudes get multiplied with two and the second half of the array get discarded. This is then plotted against the frequency bins. [6]

```

% % % % Fourier transformation of a signal % % % %
% The measured samples
xk = 51200; % Sampling frequency (Hz)
Sample_length= 2; % Sample length (seconds)
L = Fs*Sample_length ; % Length of the signal

NFFT = 2^nextpow2(L); % Next power of 2 from length of the...
...signal
Y = fft(xk,NFFT)/L; % FFT of the signal to get the amplitude
y_spec=(2*(Y(1:NFFT/2+1))); % converting from a two-sided power ...
...spectrum to an one sided power spectrum
f = Fs/2* linspace(0,1,NFFT/2+1); % Making the frequency "bins"

plot(f,abs(y_spec)) % Plotting

```

Figure 3.8: Matlab coding for a Fourier transformation

As can be seen from Figure 3.8 the frequency bins are dependent on the length of the signal. By sending in a 2 second long signal the frequency bins are 0,39 Hz while 0,5 second long signals have four times as big bins 1,5625 Hz. If the signal is uneven it can be an advantage to have bigger bins so the amplitude becomes more accurate. This was done for all the signals. The length of the signals were shorten to get bigger bins and more accurate amplitudes. The length of the signals sent in for the microphones were 0,5 seconds, instead of 2 seconds, and the length of the signals from the hotwire were 1 second instead of 4 seconds.

3.4 Nyquist theorem and quantization

Nyquist sampling theorem and the quantization of the measurements implies what to do to get good sampling data. It is important to have good sample data to get accurate measurement, and correct values when evaluating the results. If not the results will be completely off and not reliable. The Nyquist sampling theorem states that for a frequency:

$$f_s = \frac{R}{2} \quad (3.20)$$

at least R samples per seconds needs to be taken to adequately represent the signal [36, p.484]. If this amount of samples is not used aliased or under sampling can occur. Meaning that the frequencies above the Nyquist frequency are misrepresented as lower frequencies than they actually are, see the dashed line in Figure 3.9. If the sampling frequency is exactly R , it is called critical sampling. Sampling at a frequency more than twice per period is called oversampling. The normal procedure is to oversample the data which allows higher order harmonics to be detected and the signal can be down sampled if needed.

Not only does the amount of samples per seconds affect the measurements, but also how the measurements are digitalized. To assign the instantaneous amplitude sample with a binary number is called quantization. To take samples with an 2-bit quantizing process gives 4 binary numbers and 3-bit gives 8, see Figure 3.10. The bit number can easily be explained as the amount of data per wave.

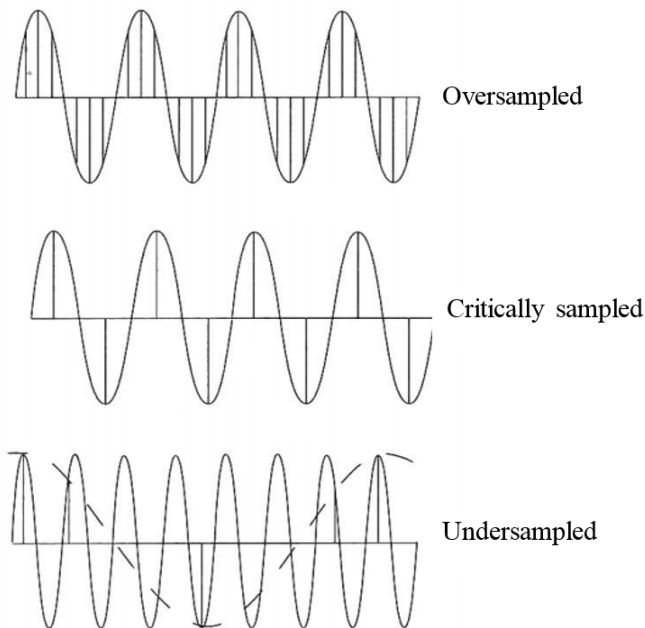


Figure 3.9: Oversampled, critical sampled and under sampled. Figure from [36, p.485]

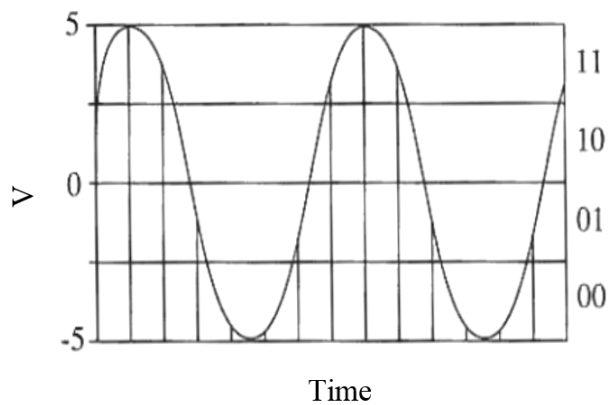


Figure 3.10: Example of 2-bit quantizer, giving 4 different values for the signal [36, p.483]

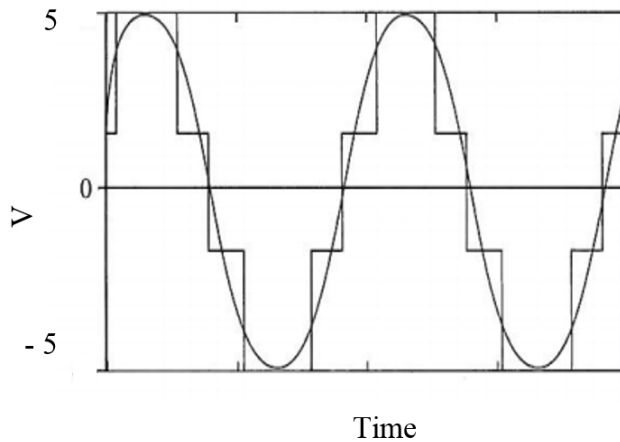


Figure 3.11: Example of changing back the signal taken by the 2-bit quantizer [36, p.484]

The number of bits, n affects the signal by dividing the signal into 2^n number of binary numbers, see Figure 3.10. More binary numbers means smaller steps when switching the signal back, see 3.11. The bigger the steps are, the bigger the error in the signal. The error in the signal should be as small as possible to get as exact signal as possible.

3.4.1 Sampling values in the experiments

The sampling frequency used for sampling the microphones was 51,2 kHz, and the length of the samples 2 seconds, clearly making it oversampling. The sampling frequency chosen was based on the maximum amount of samples the cDAQ could take, since it was possible to down sample it later. The quantization used during the microphone sampling was 24-bit, with an amplitude range of ± 5 V. The voltage resolution, or the quantization error Q is calculated by:

$$Q = \frac{\pm A_m}{2^{n-1}} \quad (3.21)$$

Where A_m is the amplitude range, and n is the number of bits. This gave a voltage resolution for the microphones $\pm 0,3 \mu\text{V}$, making the measurement very accurate.

The hotwire had a sampling frequency of 20 kHz and the length of 4 seconds, making it oversampling. The digitalization was done with a 16-bit cDAQ with a range of ± 10 V. This gave it a voltage resolution of $\pm 0,156$ mV, which was a bit high but still acceptable [36, p. 483]

3.5 Turbulent vs laminar velocity profile

A turbulent profile has a much more mean distribution of the velocity in a pipe than a laminar flow, this is caused by turbulent mixing. See Figure 3.12. This is useful when measuring with the hotwire, which requires an even velocity distribution over the wire. Therefore a turbulent flow is required when doing the measurement.

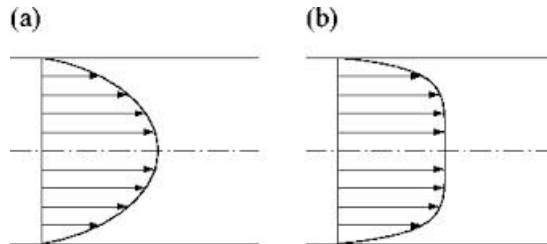


Figure 3.12: a) is an laminar flow while b) is an turbulent flow [11] [16, p.355]

To decide if the flow is turbulent or laminar it is possible to use Reynolds number:

$$Re = \frac{UD}{\nu} \quad (3.22)$$

Where U is the velocity, D the diameter and ν is the kinematic viscosity. The Reynolds number is divided into several sections:

	$Re < 2300$	Laminar flow
$2300 \lesssim$	$Re \lesssim 4000$	Transitional flow
	$Re \gtrsim 4000$	Turbulent flow

These sections are a way to decide the different states of the of the fluid without looking og testing the fluids. [16, p. 340]

Chapter 4

Preparations for the small jet

This chapter contains measurements and calibrations that was done before doing experiments with the small jet. These were essential to do to prove that the measurements in the box were done correctly and trustworthy.

The hotwire needed to be calibrated and checked to find out if the calibration was done correctly. After that a temperature control was done, to see if the calibration curve needed to be corrected for the temperature in the jet. The frequency limitation of the hotwire were investigated by a square wave test. The next step was to find the profile of the air exiting the jet, to be sure that the jet had an even flow when the air hit the hotwire. Then there were the calibration of the microphones and finding the resonance frequency of the box.

4.1 Calibration of hotwire

The hotwire needed to be calibrated before every measurement. The calibration curve could change from day to day and between the different hotwires. The calibration curve was important to have later in the experiments when the measured volts needed to be changed back to velocities.

The calibration of the hotwire was done taking measurements with different velocities from $U = 0 \text{ ms}^{-1}$ to $U = 40 \text{ ms}^{-1}$ with a 5 ms^{-1} interval. One extra point was added where $U = 0,5 \text{ ms}^{-1}$ to prevent the calibration curve from dropping below zero for low velocities. The measured voltage from the hotwire was then plotted

against the velocities in the mass flow controller. A Polyfit function from Matlab was used to find a fourth degree polynomial that fit the measured points. To be sure that the calibration was done correctly a test was done to check the reliability of the calibration curve. Can be seen in Appendix B.

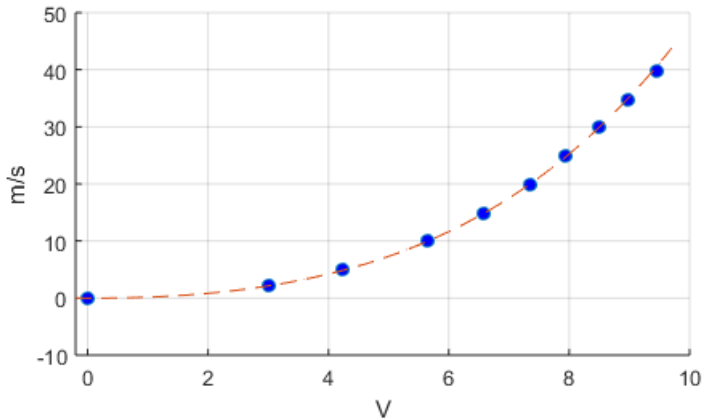


Figure 4.1: A typical calibration curve

4.2 Temperature correction

To be sure that the temperature from the jet did not change the outcome of the calibration, a temperature correction was done. A small temperature measurement device was placed right above the hotwire to measure the temperature at the jet exit, for each velocity. These temperatures were used when calibrating the curve and compared to the calibration curve without temperature correction.

As can be seen from Figure 4.2 correcting for the temperature difference between the ideal and the real temperatures was not needed, the difference were very small.

4.3 Square wave test

To find the upper limiting frequency of the hotwire a square wave test was performed. A square wave was sent through the hotwire, and the response was observed and used to calculate the frequency limit. Several hotwires were used under these experiments, and depending on the hotwire the time constant varied with

$$200\mu s < \tau_w < 750\mu s$$

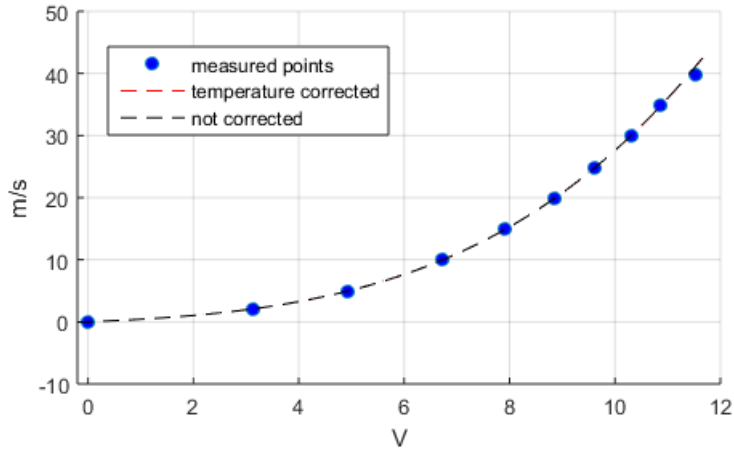
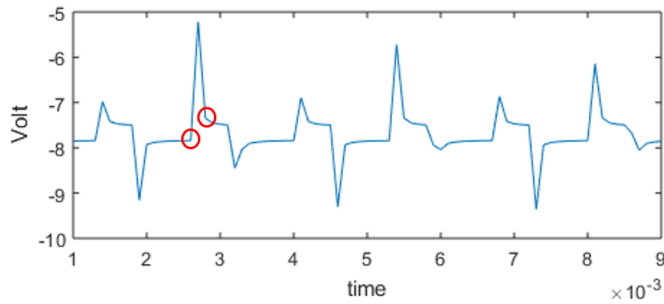


Figure 4.2: Calibration with and without temperature correction

making the limiting frequency, f_c between 1000 Hz and 3800 Hz. To be able to read where τ_w actually was 3% was very hard on an oscilloscope, so the value was read roughly at the right places just to get an approximation at which frequencies was the upper limit, the red dots in Figure 4.3

Figure 4.3: Example of a square wave test, $\tau_w \approx 2 \cdot 10^{-4}$ second

The lowest frequency of any of the hotwires were 1000 Hz meaning that any frequency measured by the hotwires above 1000 Hz was not accurate. This limited the frequency modes in the box, and only $\lambda = 2$ and $\lambda = 4$ was considered.

Notice that the peaks in Figure 4.3 are uneven, this is because the hotwire that was used to make this figure had not been properly stabilized yet. For a stabilized hotwire the peaks were even.

4.4 Jet profiles

After determine that the hotwire measured velocity correctly and finding the limitations of the hotwire, it was time to measure the jet profile. By measuring the jet profile it was possible to determine how even the velocity was as it left the nozzle. The desired profile was an even distribution, meaning that the hotwire should be able to measure the same velocity across the wire.

Three different jet profiles was measured 10 m s^{-1} , 20 m s^{-1} and 30 m s^{-1} , with $\text{Re} \approx 6600$, $\text{Re} \approx 13200$ and $\text{Re} \approx 19850$ These were all measured with a $0,5 \text{ mm}$ interval from 2 mm outside the left wall as far as 2 mm outside the right wall. Meaning that the measurements were 14 mm across the top of a 10 mm jet. 0 mm was considered the left wall and 10 mm the right wall, see Figure 4.4.

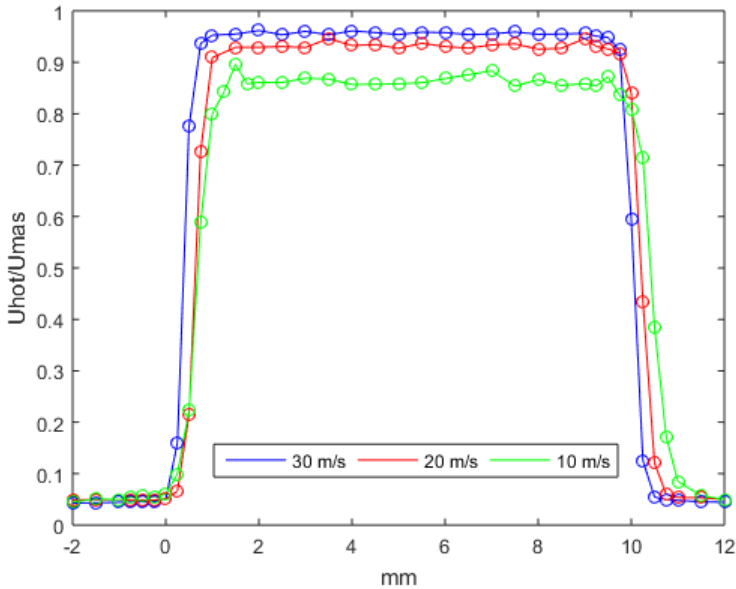


Figure 4.4: Finding the jet profiles for different velocities

$\pm 1 \text{ mm}$ from the walls the measurements were taken with 0.25 mm interval. The two first profiles, 30 m s^{-1} and 20 m s^{-1} were a lot more steady than the 10 m s^{-1} and had a velocity rate closer to 1 than 10 m s^{-1} . The velocity rate is the measured velocity U_{hot} divided on the velocity from the mass flow device U_{mas} . As can be seen in Figure 4.4 the 10 m s^{-1} velocity is closer to 0.85 than 1 and has one measured

point that is higher than the others. This higher point is most likely an error, and can be caused by inaccuracy.

This profile was the second profile that was measured across the jet, the first one is placed in Appendix C.

All three profiles from the figure clearly shows that they are turbulent, which is in accordance with the theory.

4.5 Calibration of microphones

Before starting to use the microphones, they had to be calibrated. This was done with the microphones (P1-P4/M1-M4) placed vertically in the middle of the box, 75 mm, 105 mm, 195 mm and 285 mm from the bottom. The frequency used was a resonance frequency. The lid was on during the calibration. Notice that the resonance frequencies are lower with a lid than without a lid.

Several measurements were done with 817 Hz with different amplitudes. The measured amplitudes were found by Fourier transformation, and then changed to pressure based on the sensitivity of P4 4.14 mV/Pa. The amplitudes in mV was then plotted against the amplitudes in pressure. A least squares method was used to find the lines for each microphone, and compared to each other. From the Figure 4.5 it is possible to see that all four microphones have the same line, which means that the sensitivity given from the manufacturer was correct.

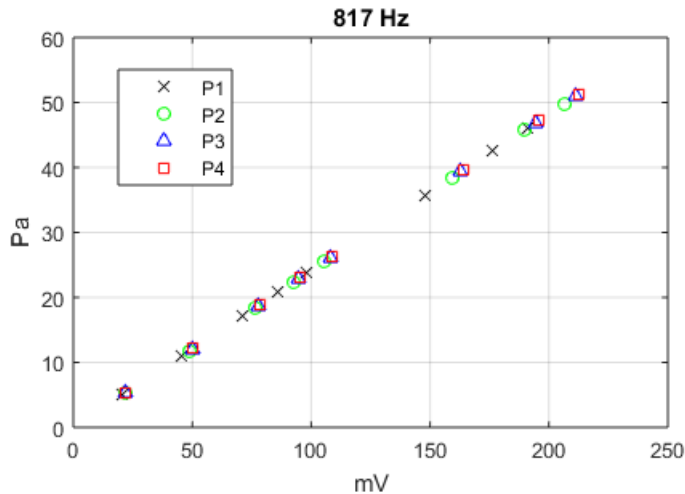


Figure 4.5: Calibration of the microphones

Notice that the microphones P1-P4 are the same microphones as M1-M4 used in the experiments for the big jet. Meaning that only microphones M1-M4 from the experiments done with the big jet are calibrated. Unfortunately the calibration of M5-M8 were forgotten before using them. Since M1-M4 and the calibration of M9-M12 in the project work all were the same as given from the manufacturer [31], it safe to say that the sensitivity of M5-M8 are the same as given by the manufacturer, and the measurements done with them are correct.

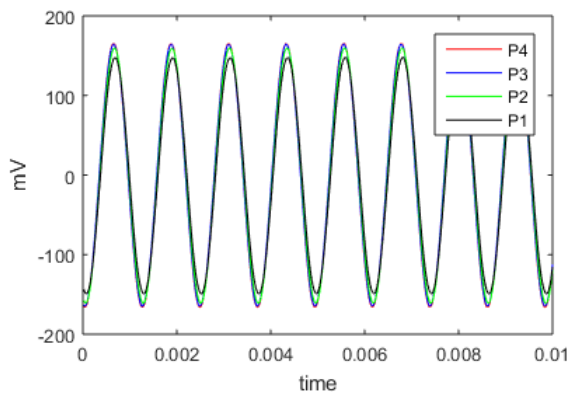


Figure 4.6: Example of corresponding time series for the four microphones. Corresponds to 150 mV in Figure 4.5

4.6 Frequencies

The frequencies that were possible to use had $\lambda=2$ and $\lambda=4$, because the antinode is at the centre of the box at these resonance frequencies. Finding $\lambda=2$ and $\lambda=4$ were done in three steps, calculating them, looking for them and a frequency sweep. The frequency sweep was done with a 50 Hz step, with the microphone placed in the middle of the box, where the antinode is. See figure 4.7. The calculated, measured and observed values are listed in Table 4.1

As can be seen from the table the frequencies that are observed and the frequencies from the frequency sweep are high compared to the calculated values. The calculated values are based on a closed box and in this experiment there is no lid. This can be the reason the real values are higher than the theoretical ones. The frequencies that were chosen to use in the next stage, was based on which frequency seemed like the strongest one. The frequencies chosen was: 452 Hz

The frequencies		
	λ	Hz
Calculated	2	398,8
	4	797,3
Observed	2	452
	4	829
Frequency sweep	2	450
	4	800-850

Table 4.1: Table over the different frequencies

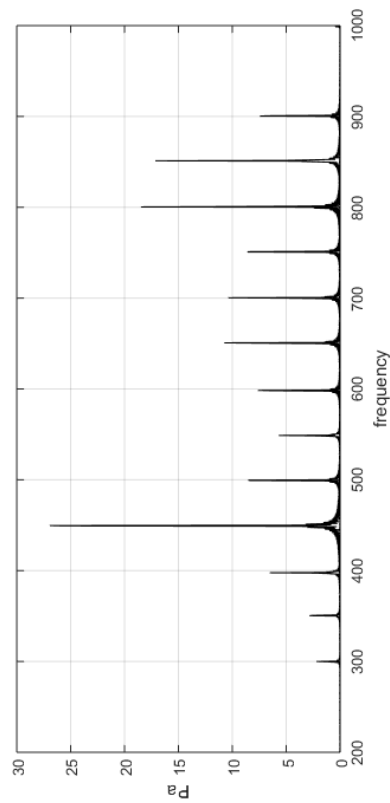


Figure 4.7: Frequency Sweep of the measured amplitudes vs frequencies

Chapter 5

Forcing of the small jet

This chapter contains the experiments with the small jet. First it describes the different positions of the jet during the experiments, after that it describes the measured velocity amplitudes and the pressure amplitudes. The next section present graphs on how the positions compare to each other and the different amplified sound signals compare to theory.

5.1 The positions of the jet

After the forcing frequency was found the next step was to decide the placement of the jet. The first position that was decided was in the middle at the antinode. 5 different positions for the jet was then chosen with equal steps between the antinode and the node, see Figure 5.1. The positions of the jet in the different positions are listed in Table 5.1

When the positions of the jet were decided, the hotwire was placed at the centre of the jet with 10 ms^{-1} air flow. Several different velocities was tried before 10 ms^{-1} was chosen, described in Appendix D. The turbulence makes disturbances that increases with the Reynolds number, and for small amplitudes these disturbances makes it difficult to measure the forcing frequency at 452 hz, therefore a lower velocity 10 ms^{-1} was chosen.

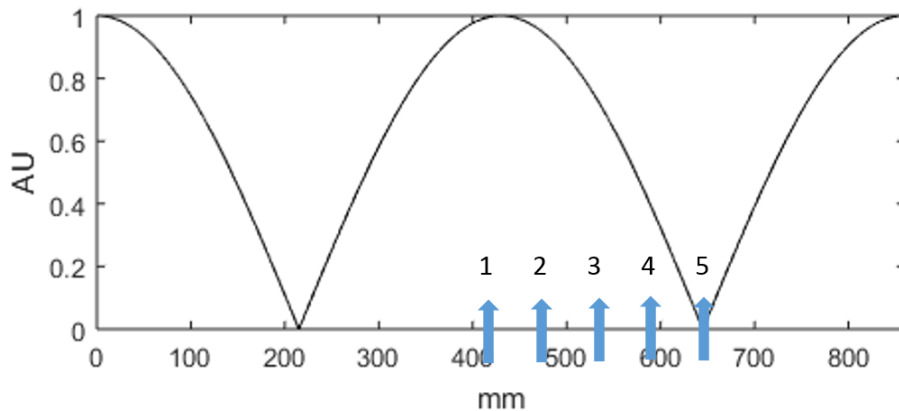


Figure 5.1: Box 860 mm, with the different positions of the jet and the sound wave

Position	Length
1 Antinode	430 mm
2	483 mm
3	537 mm
4	591 mm
5 Node	645 mm

Table 5.1: The different positions of the jet from the speaker wall

5.2 The velocity amplitudes

For the different placements of the jet, the chosen resonance frequency was producing sound while it was amplified with 11 different strengths. Were amp1 was the lowest strength and amp11 the strongest. Measurements were taken both with the microphones inside the jet and the hotwire at the jet exit. Figure 5.2 displays the measured time series for the velocities measured by the hotwire at Position 1. Figure 5.2 shows the same time series as Figure 5.3 only this have been zoomed in on the first 0,02 seconds. It displays the velocity for four different sound strengths that have been used: amp1, amp5, amp9 and amp11 at position 1.

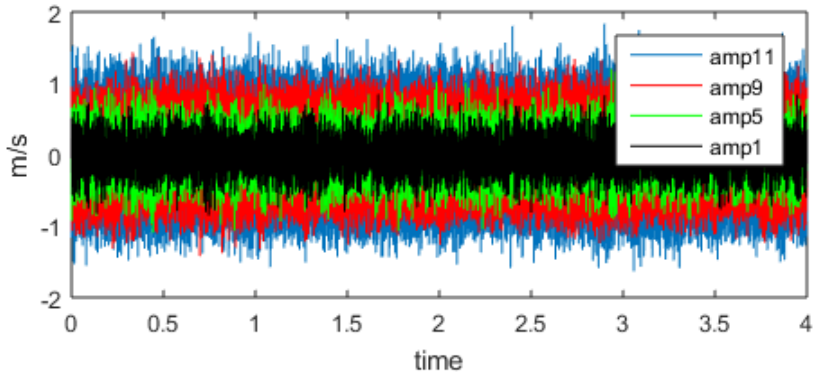


Figure 5.2: Velocity time series for position 1, showing four different forcing strengths

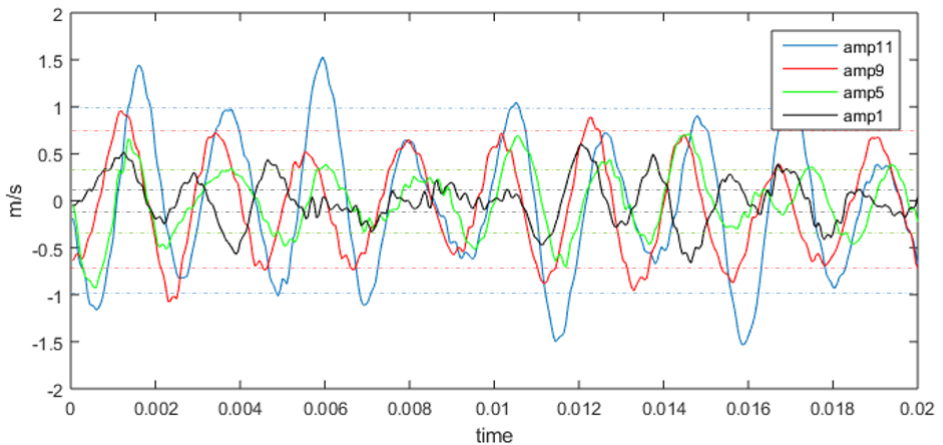


Figure 5.3: Velocity time series zoomed in for Position 1, showing four different forcing strengths

The measurements taken with the hotwire was changed into velocities and Fourier transformed to find the amplitude of the velocity at the exit. This have been listed in Table 5.4 and placed in Figure 5.3 as dotted lines. As can be seen from Figure 5.3 the amplitudes fit quite well with the time series. For the strongest amplifying strength (amp11) it is quite easy to see the forcing frequency and that the amplitude is correct. For the weakest sound strength (amp1) it looks approximately the same

size as the amp 5 in the time series, but the difference is that it is possible to detect the forcing frequency in amp5 but not in amp1, making the amplitude in amp1 weaker than amp5 even if they appear to be the same size. The measured time series for the hotwire was 4 seconds, but when the measurements were Fourier transformed only 1 second was used to get larger frequency bins and more accurate amplitudes.

Amp	Fourier transformed	
1	0.118 m/s	— · — · —
5	0.3068 m/s	— · — · —
9	0.7229 m/s	— · — · —
11	0.9676 m/s	— · — · —

Figure 5.4: Amplitudes for different sound strengths at Position 1

Notice that the amplitude of 452 Hz have been used for all the plots, even when it has not been the strongest amplitude in the amplitude spectrum. At position 5 the forcing amplitude often were lower than the amplitudes made by the turbulence, see Figure 5.5. The red circle marks the peak at 452 Hz, and is the amplitude used for position 5 amp1, even if there are other amplitudes that are stronger.

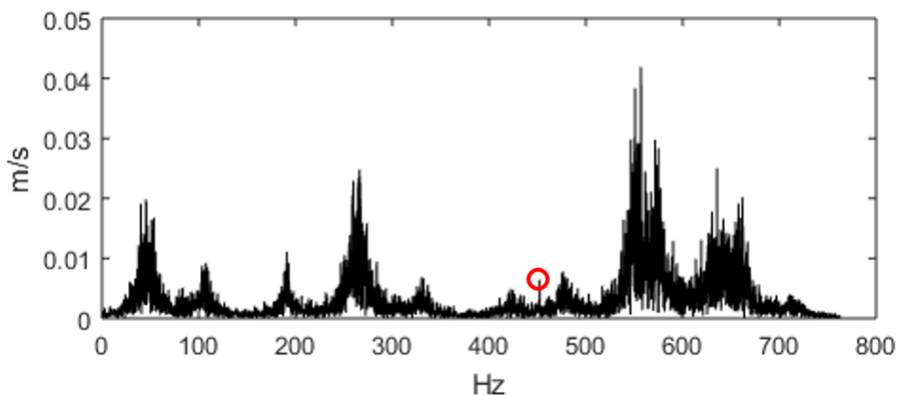


Figure 5.5: Amplitude spectrum of the measured velocities at Position 5 amp1

5.3 The pressure amplitudes

Measurements were taken by the microphones inside the jet at the same time as the hotwire measured the velocity. These measurements were changed back to pressure and Fourier transformed to find the pressure fluctuations inside the jet. Both microphones P1 and P2 were placed inside the jet, and P2 was used when making these plots.

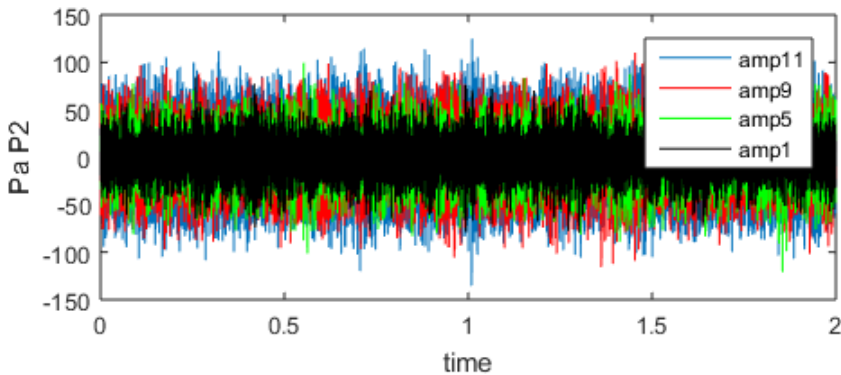


Figure 5.6: Time series of the pressure at Position 1

The pressure time series from P2 can be seen in Figure 5.6. It shows the measured pressure for four different sound levels. Figure 5.7 shows the same time series where it has been zoomed in on the first 0,02 seconds. These pressure measurements did not have a clear sinus signal as the velocity series, making it harder to decide how correct the amplitudes were. As mentioned earlier the signals that were Fourier transformed were cut down from 2 seconds to 0,5 seconds to make the bins larger and the amplitudes more accurate.

The numbers and the colours in Table 5.8 correspond to the dotted lines in Figure 5.7. The dotted lines are the Fourier transformed amplitudes and shows the size of the amplitudes compared to the signals.

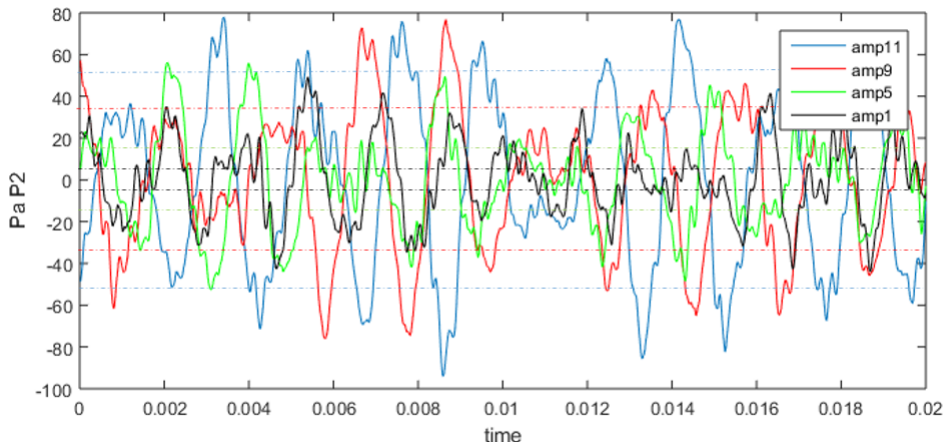


Figure 5.7: Time series of the pressure from P2 zoomed in, with the Fourier transformed amplitudes marked as dotted lines

Amp	Fourier transformed
1	5.68 Pa - . - . -
5	16.01 Pa - . - . -
9	36.45 Pa - . - . -
11	50.02 Pa - . - . -

Figure 5.8: P2 and the amplitudes of the different sine waves

5.4 The Positions compared to each other

The different amplitudes from the microphones and the hotwire were plotted against each other. They form a straight line which is reasonable since higher pressure fluctuations makes higher velocity fluctuations. As can be seen from Figure 5.9 it is not a perfect straight line, amp8 is a bit low and amp4 is a bit high. The colours of amp1, amp5, amp9 and amp11 corresponds to the colours in Figure 5.7 and Figure 5.3 , and the amplitudes in Table 5.2. The graph still makes a good representation of the measurements taken and shows that there is some inaccuracy.

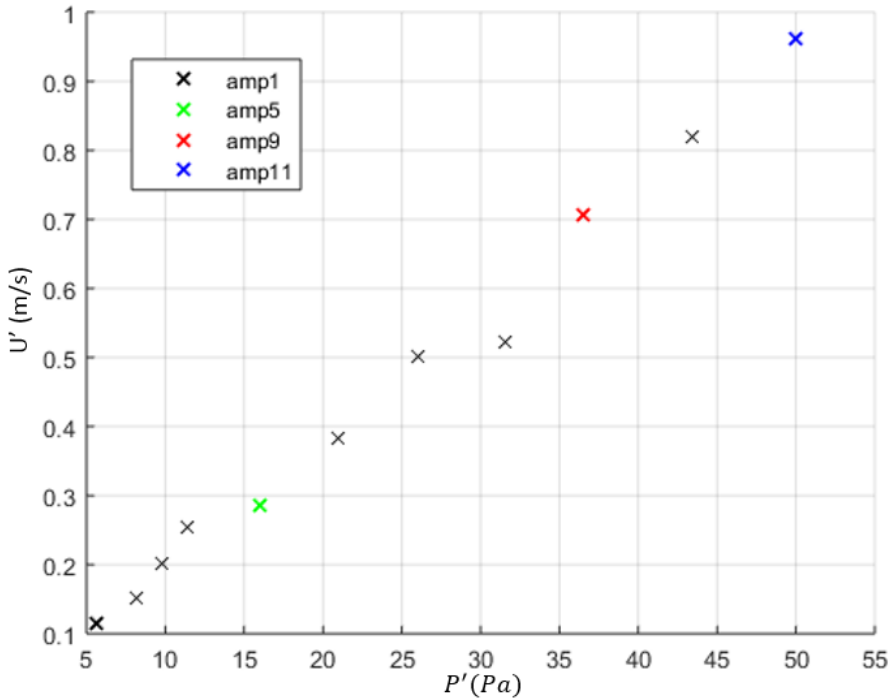


Figure 5.9: Position 1 velocity amplitude vs pressure amplitude

Amp	Amplitude P2	Amplitude Hotwire
1	5,68 Pa	0,118 m/s
5	16,01 Pa	0,3068 m/s
9	36,45 Pa	0,7229 m/s
11	50,02 Pa	0,9676 m/s

Table 5.2: The velocity amplitudes and the pressure amplitudes

All the different positions were plotted in the same graph were the x-axis and the y-axis were made dimensionless. The velocity amplitudes U' were divided on the velocity $9.97 \text{ ms}^{-1} \bar{U}$, and the pressure amplitudes P' were divided on the atmospheric pressure $101,1 \text{ kPa} \bar{P}$.

It is reasonable that position 1 has the strongest amplitudes and position 5 has the weakest. Position 5 is at the node where the pressure amplitudes are the weakest

and position 1 is at the antinode where the pressure amplitudes are the strongest. As can be seen from Figure 5.10 all the positions form the same straight line, meaning that the gradient is the same for all positions. It is clear that the size of the pressure fluctuations from the speakers affect the velocity amplitudes in the jet, and that the pressure amplitudes make the velocity from the jet oscillate.

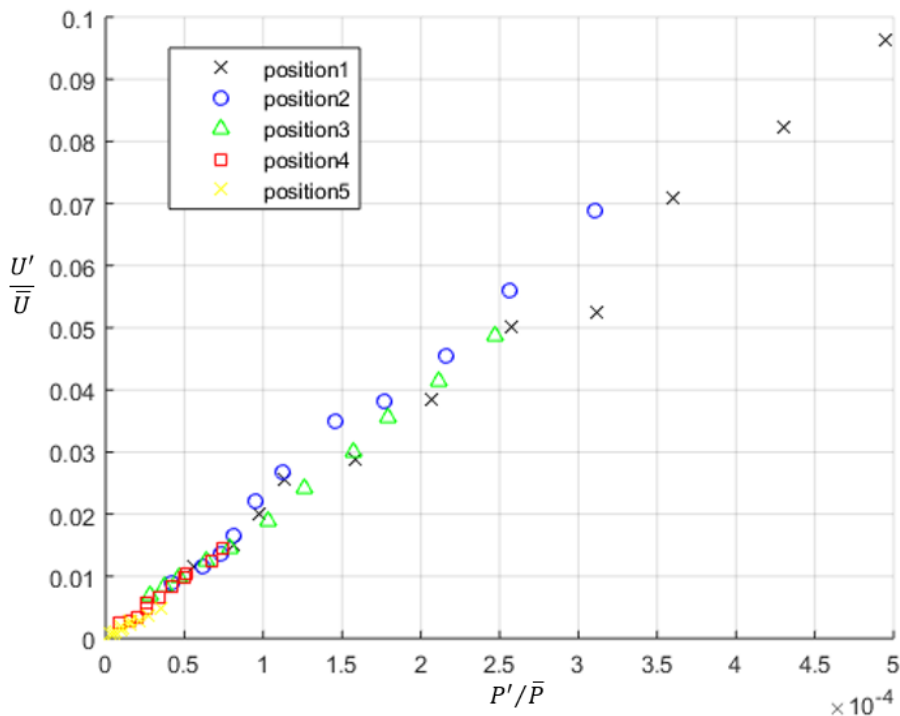


Figure 5.10: The different positions compared to each other

The largest variation can be seen in Position 1 with the strongest amplitude Amp11. This sound level has almost 20 % velocity variation compared to the constant velocity. This is a lot. 20 % variation in the speed created by the resonance frequency at the strongest amplitude, compared to 2% for the weakest at the same position. At the node the velocity variation is 1% at the weakest and 1% at the strongest. If these variations had been even stronger at the antinode they could affect the direction of the velocity. 20% variation in the velocity, means 11 ms^{-1} when the pressure amplitudes amplifies the velocity, and 9 ms^{-1} when it cancels the velocity. When strong enough they can clog the air, or “plugging” the velocity flow rate [22].

Figure 5.11 shows the same as Figure 5.10 only the two last positions are zoomed in, since they are a bit smaller than position 1, 2 and 3. It is possible to see that these positions also are linear, but the measurements are more uneven. It even looks like the measurements from position 5 does not have as steep gradient as position 4. The reason the linearity is not accurate close to the node compared to the antinode might be that the speakers are uneven. This is observed later in section 6.1.1. They do not propagate the exact same amplitude, and this can be observed close to the node. That the measurements done in position 5 forms a straight line indicates that the node is not exactly at the centre of the jet, but that it is slightly to the side

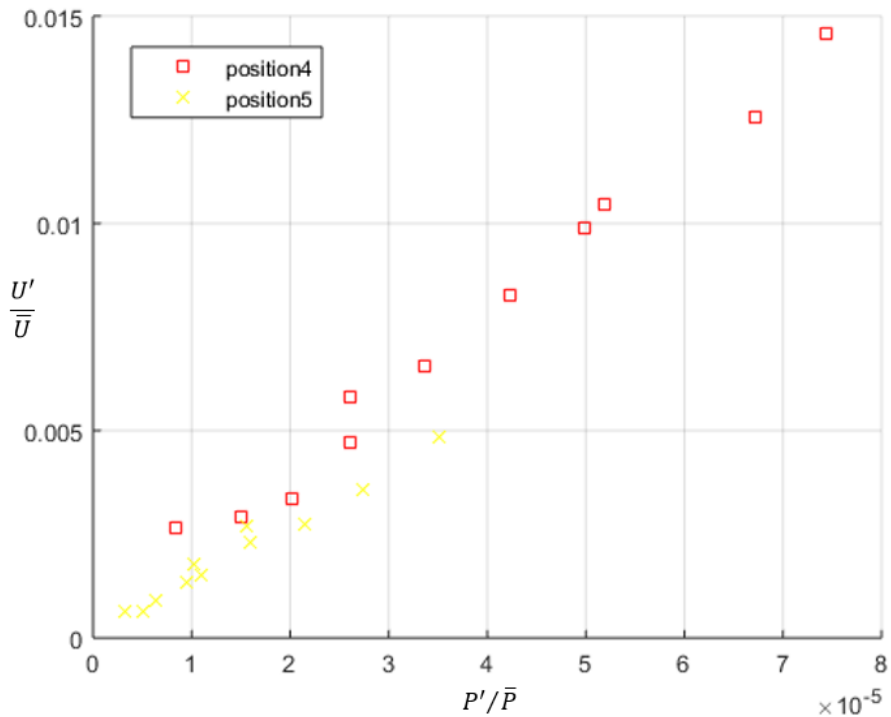


Figure 5.11: Position 4 and 5 zoomed in

5.5 Comparing results with theory

To check if the graphs were correct, four different sound levels amp1, amp5, amp9 and amp11 were plotted against different positions in the box. According to theory these measurements should make 1/4 of a sine wave, the absolute sine wave as can be seen in in Figure 5.12. By comparing Figure 5.12 and Figure 5.13 the lines in Figure 5.13 are more straight than curvy, but they are roughly the same. Amp1 looks right, while all the other amplified levels seem to be a bit low at position 2 and 4, especially in position 2.

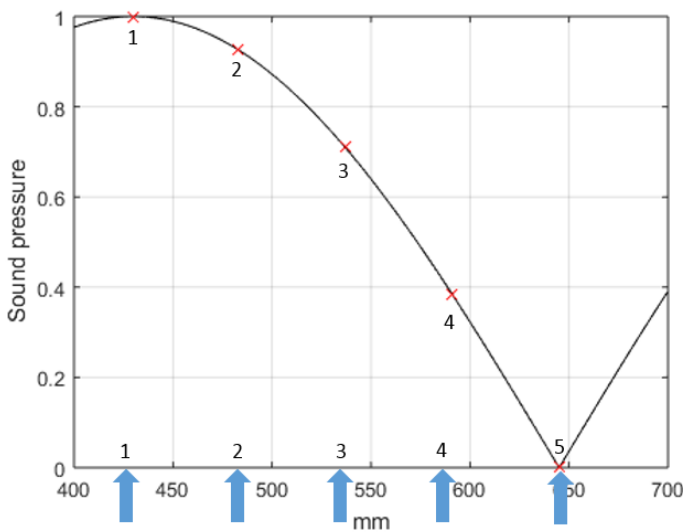


Figure 5.12: The different positions of the jet and the pressure amplitudes that should be measured at the different positions

The velocity amplitudes were also plotted against the positions see Figure 5.14, and should have the same shape as the pressure, which they do. Even the same inaccuracies can be seen. Position 2 and position 4 are lower than the others like for the pressure amplitudes.

All four strengths from both velocity and pressure compare quite well with the theory. This indicates that all the measurements done with small jet are correct, and that the measurements are reliable. If something had been wrong this would most likely reveal it.

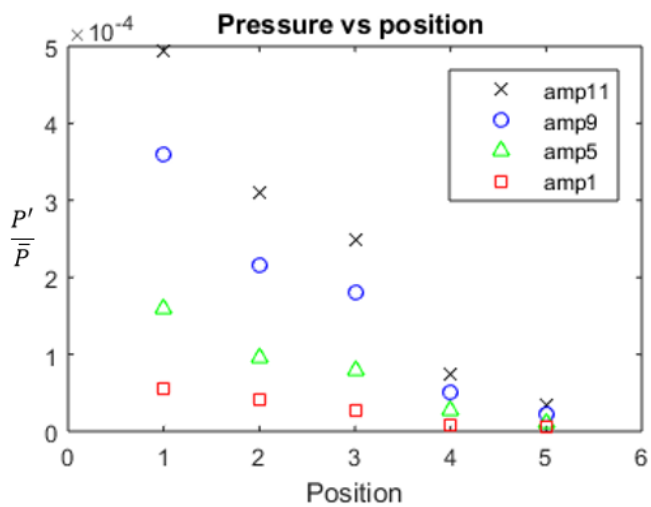


Figure 5.13: Pressure amplitude divided on the pressure vs the position of the jet

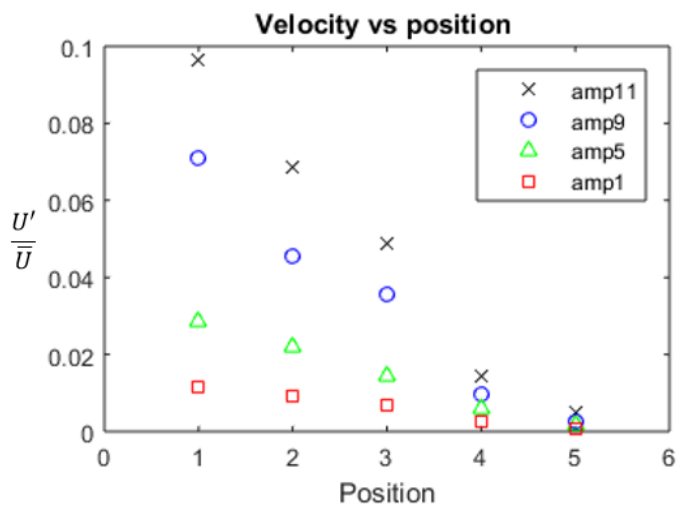


Figure 5.14: Velocity amplitude divided on the velocity vs the position of the jet

Chapter 6

Forcing of the big jet

This chapter contains the experiments with the big jet. The point with this experiment was to place the node at the centre of the jet and measure the pressure changes inside the big jet. Only frequency modes with an uneven number have the node at the centre of the box, for even mode numbers the antinode is at the centre, therefore there was not so many mode numbers to choose between.

Two different mode numbers were used:

$$\lambda = 3 \text{ and } \lambda = 5$$

$\lambda = 1$ and $\lambda = 7$ was also considered, but to achieve $\lambda = 1$ a frequency of approximately 200 Hz was needed, this was too low for the speakers. $\lambda = 7$ was too high to be considered relevant, see Table 6.1

The first step was to calculate the frequencies:

Calculated frequencies		
λ	Frequency	
1	200	Hz
3	600	Hz
5	1000	Hz
7	1400	Hz

Table 6.1: The different calculated frequencies

6.1 Low forcing frequency

To determine the actual frequencies, the four microphones on the wall were used (M9-M12). The amplitudes from these microphones could be used to find the resonance frequency by comparing them to the theoretical ones.

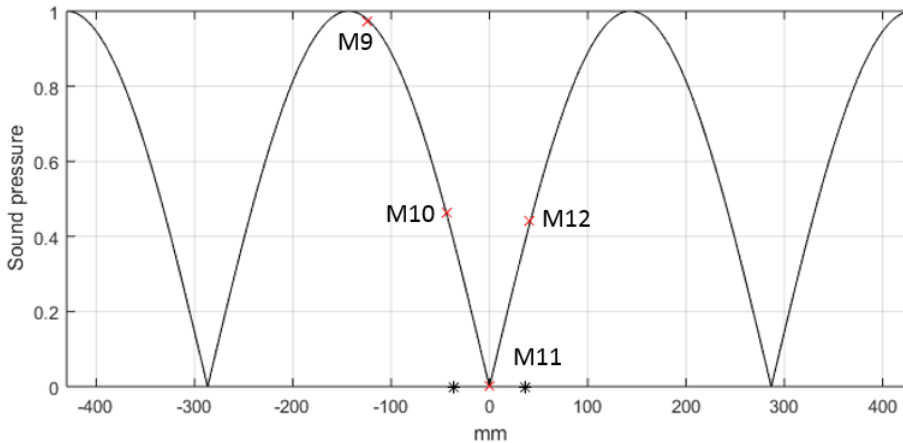


Figure 6.1: The different amplitudes the microphones on the wall should measure when $\lambda = 3$

Figure 6.1 shows the placement of the microphones in the x direction, and the sound pressure from the resonance frequency $\lambda = 3$ in the y direction. The red crosses are the microphones, and should measure the amplitudes compared to each other as they display in the figure. This means that M9 is almost at the antinode, and should be as high as possible. M10 and M12 are almost the same distance from the node, and should measure the same amplitude, but 180° out of phase. M11 is placed at the node and should display a small amplitude, preferably only a straight line. The black stars at the bottom represent the jet walls. The most powerful frequency observed was 633 Hz. The time series of this frequency can be seen in Figure 6.2.

As can be seen from Figure 6.2 the amplitudes fit quite well with what was predicted. M10 and M12 are approximately the same size, but 180° out of phase. M11 was not a straight line, but as small as it was possible to get it and M9 were the strongest. Notice that there is a phase difference of 42° between M9 and M11. This phase change should not occur.

When this frequency was found the readings from the microphones in the big jet

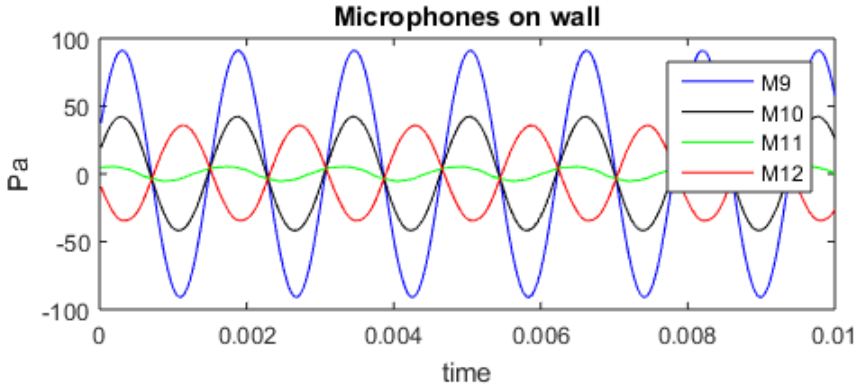


Figure 6.2: The measured amplitudes from the microphones on the wall with frequency 633 Hz

were looked at, see Figure 6.4. These showed that something was not right. The same phase shift that occur in M11 on the wall occur on the microphones in the jet. Theoretically M3 and M7 should be 180° out of phase and of equally size. The phase shift between M3 and M7 was calculated to 83° . M1 and M5 should be at the node, and ideally a straight line. That was not the case. From Figure 6.4 it looked like the node was closer to M3 than M7. Some experimentation with moving the walls were done to see what moving the node would do for the measurements. This can be seen in Appendix E.

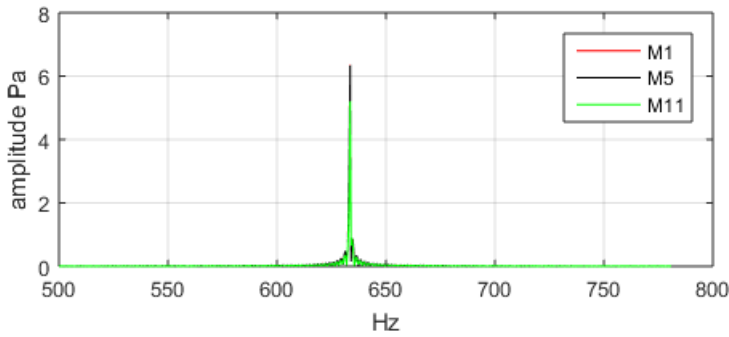


Figure 6.3: Amplitude spectre for M1, M5 and M11

To be sure that the measurements on the wall and the measurements in the jet were done correctly, the amplitudes and the frequencies from M1, M5 and M11 were compared. They should measure the same. M1 and M5 are exactly the same

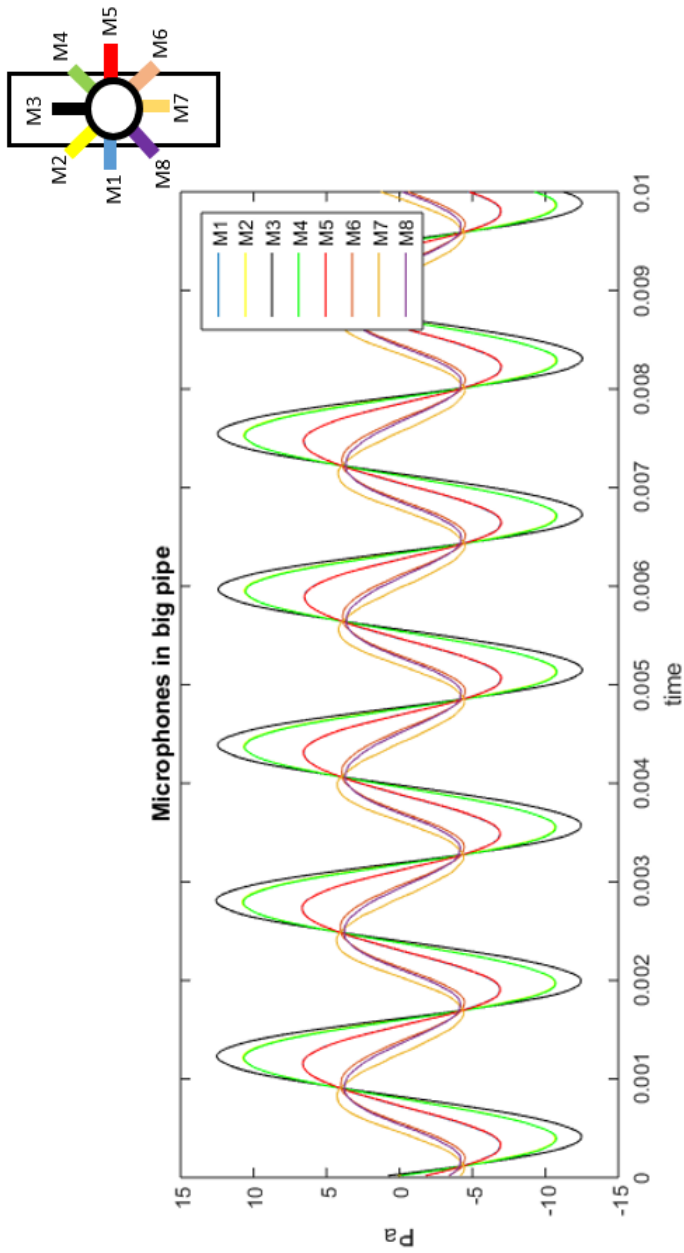


Figure 6.4: The amplitudes measured by the microphone inside the jet

6.3 Pa, while M11 has 5.2 Pa. See Figure 6.3. This was close enough to consider the measurements taken inside the jet and the measurements taken on the wall to be correct.

The microphones on the wall M10 and M12 are placed very close to the jet wall on each side, ideally they should have the same amplitude as M3 and M7. There is a big difference in these amplitudes. M3 has an amplitude of 13 Pa and M7 has 5 Pa, M10 and M12 have an amplitude of 41 Pa and 35 Pa. This was not a good sign but the amplitudes measured at the node both on the wall and in the jet were the same, indicating that there could be another reason for the difference. A reason that they do not measure the same pressure might be that the orientation of these microphones are different, or the heights are different. M3 and M7 are placed parallel to the speaker walls, while M10 and M12 are perpendicular to the speaker walls.

6.1.1 Why not as predicted

The reason the measurements with the microphones were not as expected are most likely because the speakers have a small difference in the amplitudes. This difference is only visible close to the node. At the antinodes the amplitude difference is so small that the difference does not affect the total sum of the signals, and they behave as the theory.

To see if the difference in the sine signals can have an affect on the phase a Matlab script was created with two different sine signals travelling in the opposite direction with different amplitudes, see Figure 6.6. The red sine signal is the sum of the green travelling to the left and the blue travelling to the right. It can be seen from the red signal at the different time positions that the phase of the red sine signal moves with the green signal, which has the largest amplitude.

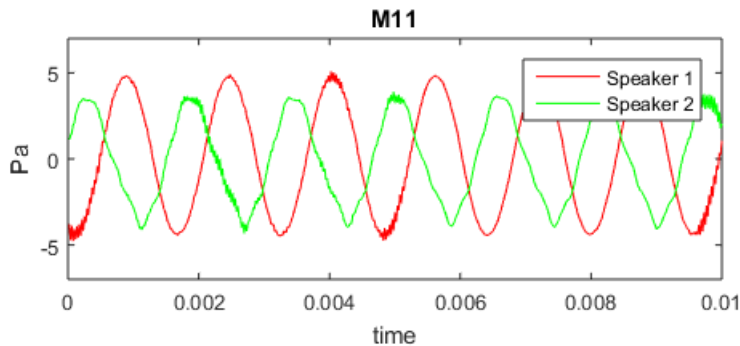


Figure 6.5: Measuring the speakers at the node, using M11

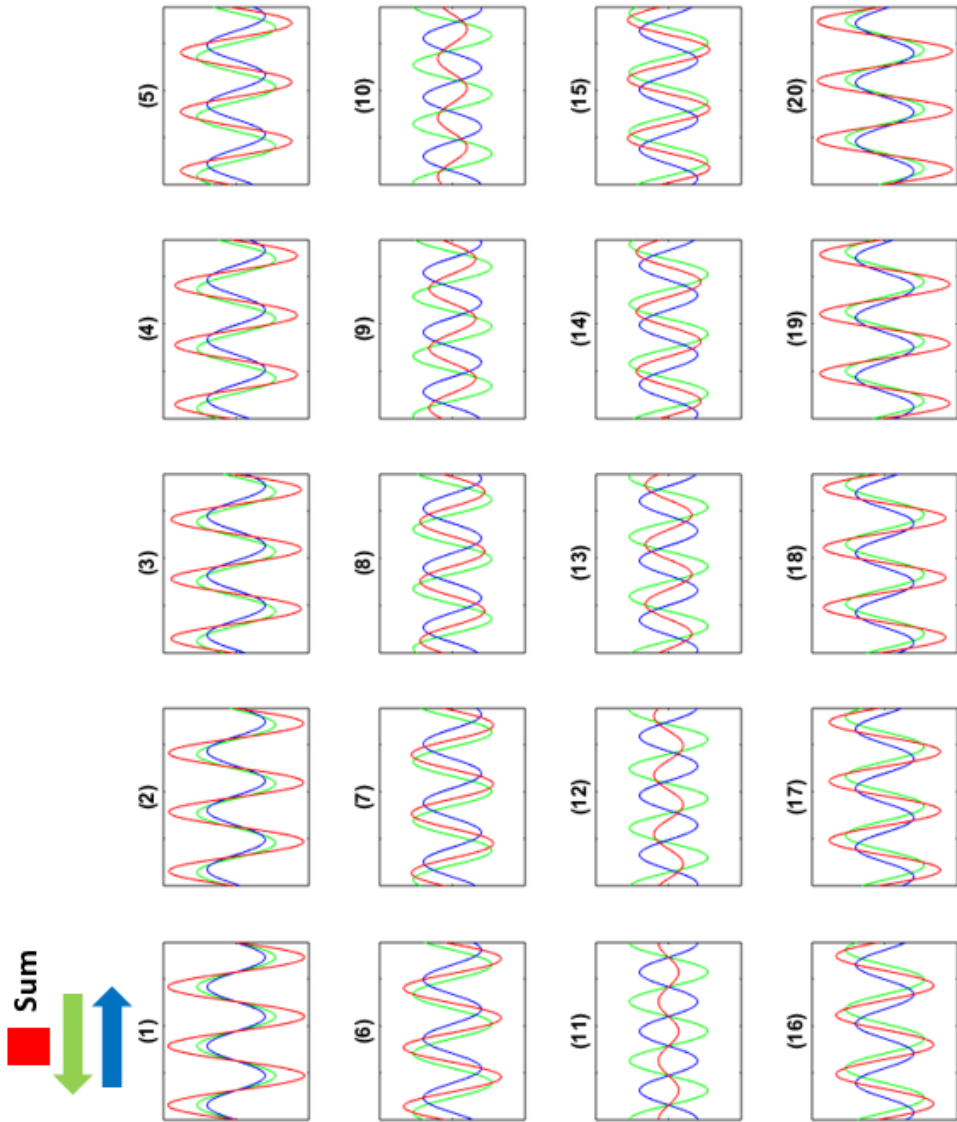


Figure 6.6: Simulation of sine signals travelling in the opposite direction, with different amplitudes

The red signal does not behave as an ideal resonance frequency. In sub-plot 1 the signals reinforce each other and in sub-plot 11 the signals cancel each other out. As can be seen from sub-plot 11 the signals do not cancel each other out completely, and the red does not have fixed nodes or antinodes.

To see if there were any amplitude difference from the speakers, each speaker was measured at the node individually. This can be seen in Figure 6.5. By Fourier transforming them, the amplitudes measured by M11 for both speakers was revealed to be 2.7 Pa and 3.6 Pa. This does not prove that the amplitudes in the speakers are different, since sound reflection from the other wall can alter the measurements, but it strongly indicates that it is the case.

6.1.2 With airflow

After all the measurements in the jet without airflow it was time to take the same measurements with airflow. The Reynolds number used was the same as in the small jet, making the exit velocity $1,36 \text{ ms}^{-1}$. The time series for the 8 microphones in the jet are displayed in Figure 6.7 and a zoomed time series can be seen in Figure 6.8.

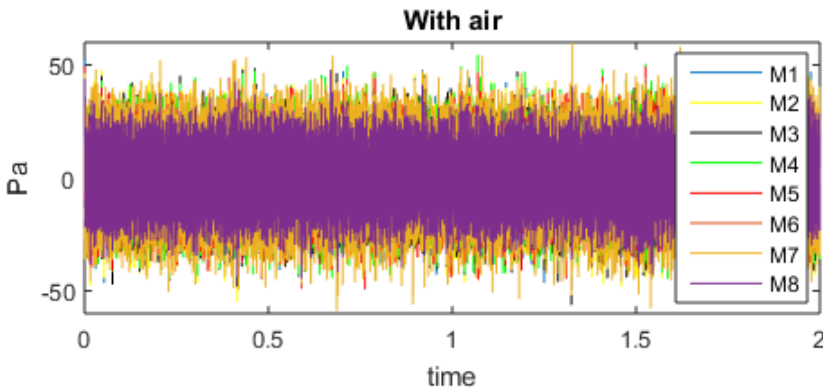


Figure 6.7: The time series from the microphones inside the jet

The airflow makes it impossible to see the original sine signals from the speakers, but by calculating the amplitudes from the forcing frequency see Table 6.2, it is possible to compare the results. The difference between the measurements with airflow and the one without airflow is minimal. The amplitudes are roughly the same. A corresponding amplitude spectrum of M7 is provided in Figure 6.9. The amplitude spectrum shows that the air makes velocity disturbances with small amplitudes.

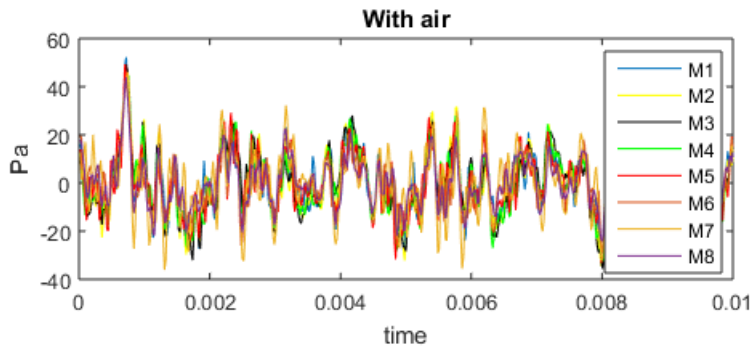


Figure 6.8: The time series from the microphones inside the jet zoomed in

Amplitudes for the forcing frequency				
	Without airflow		With airflow	
M1	6,3	Pa	6,8	Pa
M2	10	Pa	10,6	Pa
M3	11,7	Pa	12,3	Pa
M4	10	Pa	10,6	Pa
M5	6,3	Pa	6,8	Pa
M6	4	Pa	4,2	Pa
M7	4	Pa	4,1	Pa
M8	3,7	Pa	3,9	Pa

Table 6.2: The amplitudes from the microphones inside the jet, with and without airflow

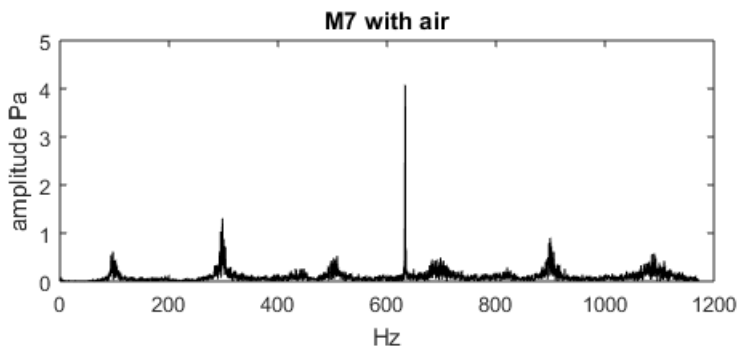


Figure 6.9: The amplitude spectrum of M7 with air

6.2 High forcing frequency

The first step was to find the resonance frequency for $\lambda = 5$, this was done by observation. As can be seen from Figure 6.10 M9 was the microphone closest to the antinode, and had the largest amplitude of the microphones. M10 and M12 were approximately the same size and 180° out of phase. The jet walls are marked as black stars in the figure. M11 was at the node and should be as small as possible. When the wanted frequency of 1000 Hz was found, the microphones inside the jet were used.

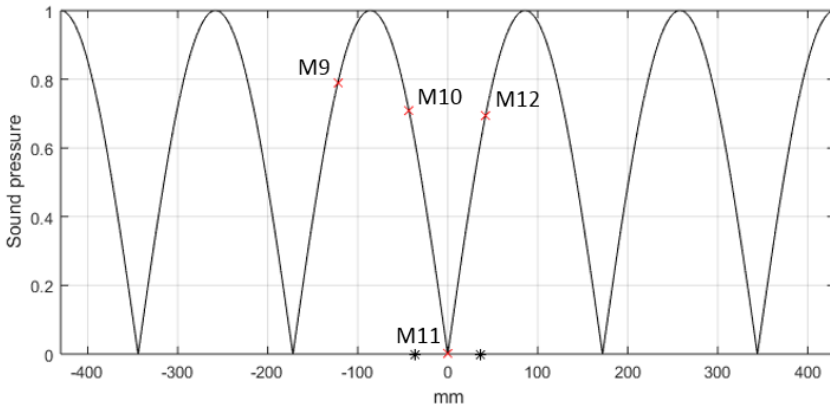


Figure 6.10: The amplitudes on the wall when $\lambda = 5$, compared with each other

As can be seen from Figure 6.11 the expected phase shift from the theory occurs. But the amplitudes in M3 and M7 should be the same size, meaning that the node is not at the exact centre of the jet. Therefore the walls were moved slightly until the amplitudes of M3 and M7 were the same size. See Figure 6.12. From this figure it is possible to see that the measurements fit quite well with the theory. M2 and M4 measure the same amplitude as M6 and M8 except that they are 180° out of phase. This means that the phase shift does not affect any other place than at the very centre, the node M1 and M5. This phase shift around the jet is also observed in the work of O'Conner and Lieuwen [33] and O'Conner et al. [26] where the phase on the right and the left side of the burner oscillates out-of-phase when the pressure node is at the centre. This indicates that the measurements are correct.

The microphones on the wall were then used again to measure the amplitudes of this new position. The time series of this measurement can be seen in Figure 6.13. These amplitudes fit quite well with the size of the amplitudes from Figure 6.10. M9 has the largest amplitude, M10 and M12 have the same size, were they are

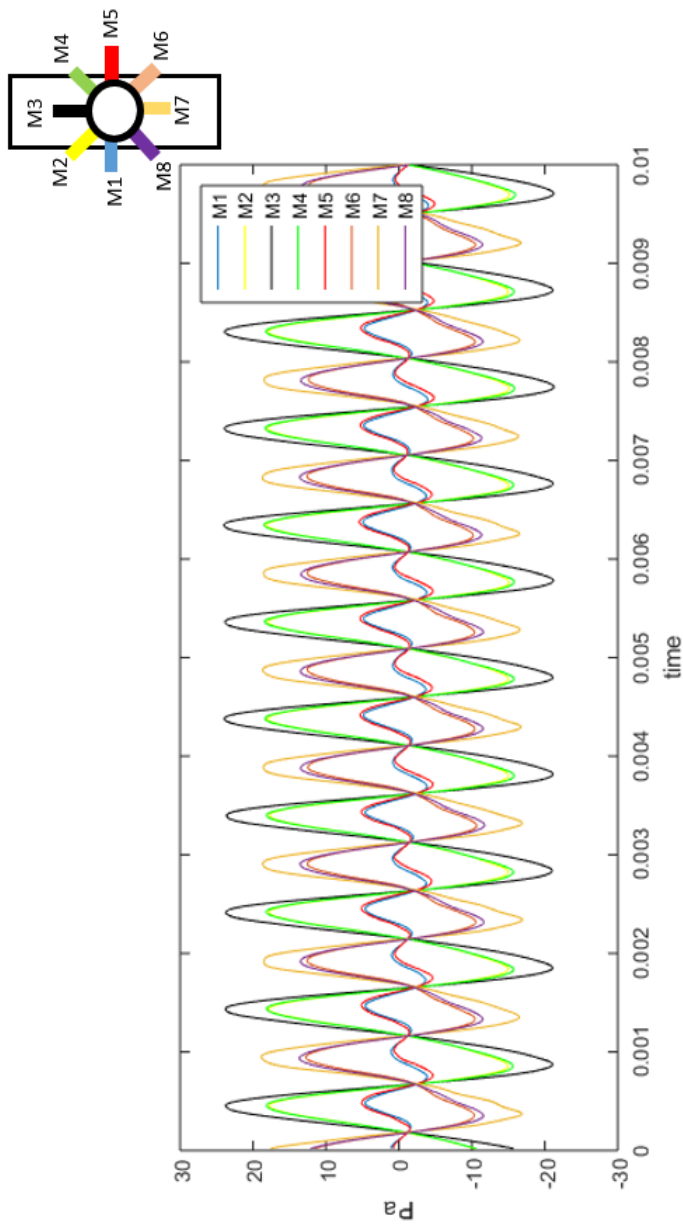


Figure 6.11: The time series of the microphones inside the jet before moving the walls

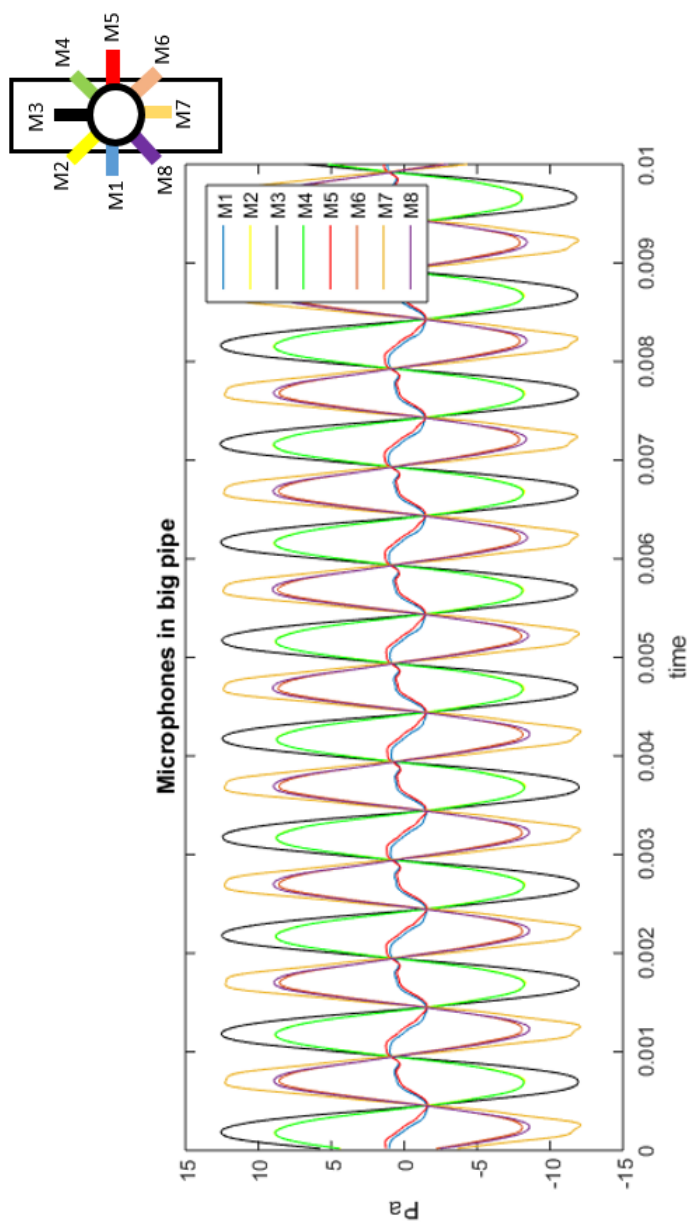


Figure 6.12: The time series of the microphones inside the big jet

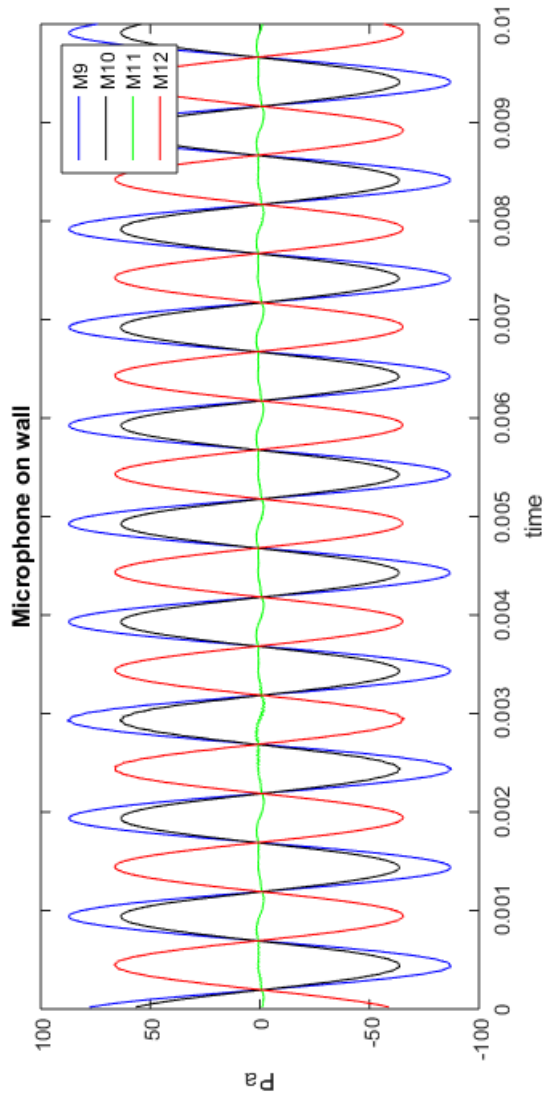


Figure 6.13: The time series of the microphones of the wall

180° out of phase and M11 is extremely small. The Phase shift that was seen when $\lambda = 3$, can not be seen here except for M1, M5 and M11 which is at the exact node. The phase shift here between M9 and M11 was 29° which is a bit lower than for $\lambda = 3$, 42°.

The amplitude from M11 at the node on the wall was compared to the amplitudes measured by M1 and M5 inside the jet. As can be seen from Figure 6.14, the shape and size from the three microphones compared quite well. By Fourier transforming the signals it was possible to see that the three measured signals was almost identical. The amplitudes from these three microphones were the same, see Figure 6.15. This indicated that the measurements from the wall and the measurements from the jet were done correctly.

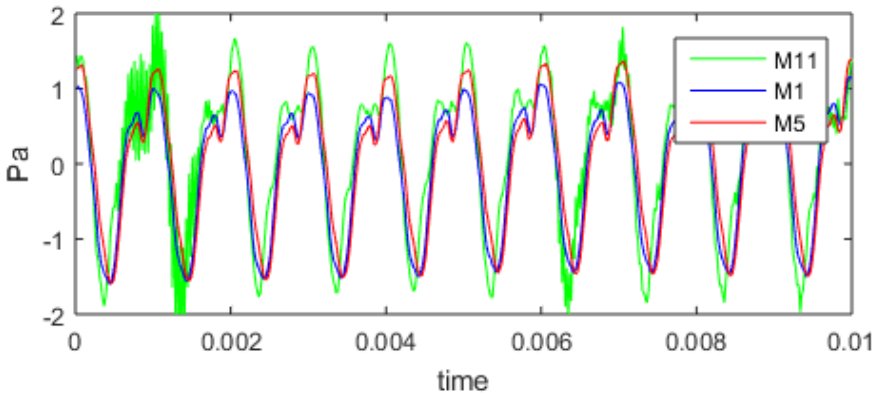


Figure 6.14: The time series for M11, M1 and M5

The microphones on the wall M10 and M12 are placed very close to the jet walls on each side. Ideally they should have the same or a similar amplitude as M3 and M7, but there are a big difference in these amplitudes. As mentioned earlier the reason that these might not be the same, could be the direction of the microphones.

A reason that the measurements with $\lambda = 5$ were closer to the theory could be that the gradient is steeper for $\lambda = 5$ than for $\lambda = 3$. This makes the difference between the speaker amplitudes relatively smaller for the same positions. The smaller the difference between the sine signals are, the less it affects the sum. This might be the reason that the phase shift can only be observed at the very centre.

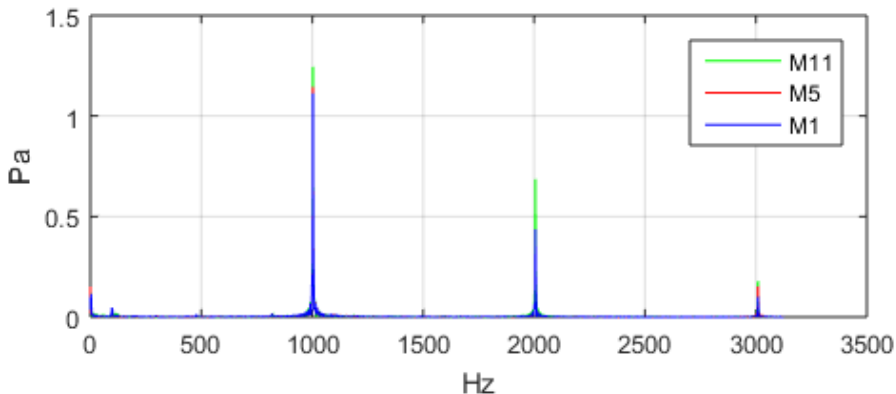


Figure 6.15: Amplitude spectrum for M11, M1 and M5

6.2.1 With airflow

After the measurements without airflow, it was time to do the same with airflow. The time series for the microphones inside the jet can be seen in Figure 6.16. The original sine signals can not be observed, since the air makes disturbances. But by comparing the amplitudes of the forcing frequency with the amplitudes of the signal without airflow, it is possible to see the similarity. Table 6.3 displays the different amplitudes from the two different measurements. The size of the amplitudes are close to each other, and indicates that the airflow makes a small difference.

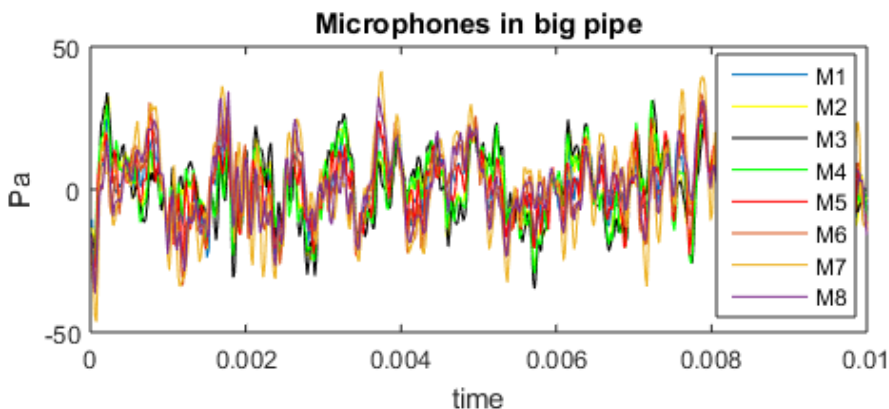


Figure 6.16: Time series for the microphones inside the jet with airflow

Amplitudes for the forcing frequency				
	Without airflow		With airflow	
M1	1,1	Pa	0,9	Pa
M2	7	Pa	7,4	Pa
M3	10,2	Pa	10,6	Pa
M4	7	Pa	7,4	Pa
M5	1,1	Pa	1	Pa
M6	7,2	Pa	6,7	Pa
M7	10,5	Pa	10	Pa
M8	7,6	Pa	7,2	Pa

Table 6.3: The amplitudes from the microphones inside the jet with and without airflow

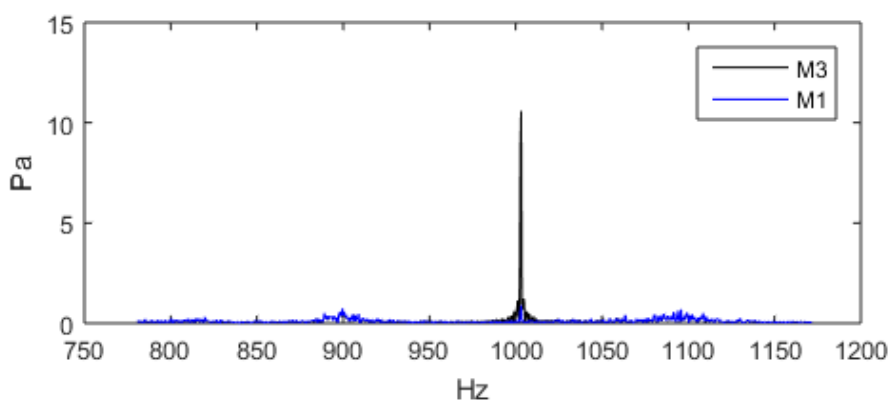


Figure 6.17: Amplitude spectrum for M1 and M3 with airflow

Figure 6.17 displays the corresponding amplitude spectrum to microphone M1 and M3 with airflow. The disturbances from the airflow makes the amplitude of the forcing frequency of M1 just slightly bigger than the other amplitudes, making it hard to distinguish from the other peaks. M3 on the other hand is easy.

Chapter 7

Conclusion and future work

7.1 Experimental uncertainties

Several uncertainties can make the measurements inaccurate. Random errors, inaccurate measurements and mistakes in the calculations can occur. These uncertainties can affect the results, and the most obvious uncertainties not already mentioned will be commented in this section.

7.1.1 Measurements

The settings on the frequency generator were not digital. This made it unstable and imprecise when tuning in on a specific frequency. It often fluxed a little bit while staying on one frequency and it was difficult to tune in on one frequency and hold it stable there. This probably made the signal which were used to force the jets ± 0.5 Hz accurate. This again affects the accuracy of the measured amplitudes, and later when Fourier transforming the signals to find the amplitudes.

The measurements done on the placement of the microphones on the walls are inaccurate. They were difficult to measure precisely, and the pipes that are holding the microphone in place have a diameter of 1-2 mm bigger than the microphones making the placement of the microphones inaccurate.

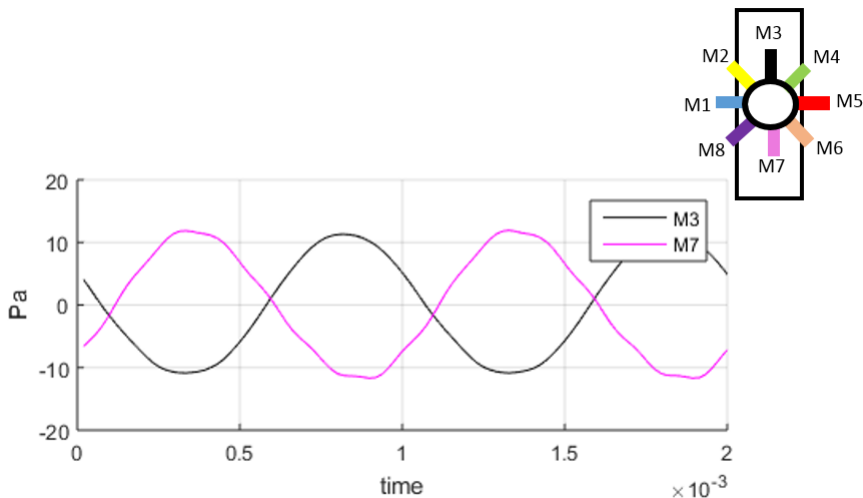


Figure 7.1: Time series $\lambda = 5$, M3 and M7, the microphone closest to each speaker

7.1.2 Accuracy of the signals

As can be seen from Figure 7.1 the sine signals from microphone 3 and 7 from the big jet $\lambda = 5$ does not cross at zero. This was a problem for some of the measured signals. If these were perfect standing waves they would cross each other at zero. This affect the accuracy of the signals, but this influence is probably so small that it can be neglected.

The sizes of the frequency bins affect the results from the Fourier transformation more than imperfect standing waves. Larger bins collects more of the signals, and makes the amplitudes more accurate. This is not necessary if the sine signals are even, but if they are uneven (see Figure 7.2) the size of the bins can have a large impact on the result. The signal used in Figure 7.2 has the strongest amplitude (amp11) from the small jet in position 1. For the small bins the amplitude is 40 Pa while for the big bins it is 50 Pa. Making bigger bins than 1.56 Hz or sending in a shorter time series than 0.5 seconds did not make a big difference in the amplitude. Therefore 0.5 seconds was considered an acceptable size of the bins, but there is some small difference anyway. Making bigger bins, especially when the frequency generator fluctuates a bit up and down when using it, can have a huge impact on the Fourier transformed amplitudes. The same was for the hotwire.

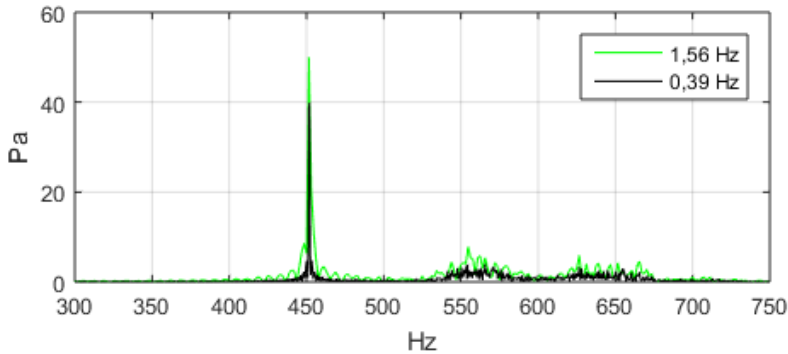


Figure 7.2: Two different sizes of the frequency bins same signal

7.2 Conclusion

To summarize this master thesis:

Small jet

- I have learned how to make hotwires, calibrate them and how to use them in combination with microphones.
- The amplitudes measured at the antinode were the strongest and the amplitudes measured in the node were the weakest.
- The measured pressure amplitudes inside the jet were linear to the velocity amplitudes measured by the hotwire at the exit.
- The gradient in the graph where the velocity and pressure amplitudes was plotted, were the same for all five positions.

Big jet

- The measurements done with a low resonance frequency did not match the theory because the speakers have a small difference in the amplitudes.
- The measurements done with a higher resonance frequency did match the theory.
- The measured pressure amplitudes was of equal size and 180 ° out of phase in the direction the sound was propagating, for the higher resonance frequency.
- The measured pressure amplitudes for the forcing frequency does not change size when using air in the jet.

7.3 Recommendations for further work

Recommended further work on the small jet would be to do measurements of multiple jets arranged in an annulus. This could be used to compare with the single transverse jet experiments.

The next part in the big jet would be to take PIV measurements of the node for both $\lambda = 3$ and $\lambda = 5$ and see how it behaves. Another idea would be to do the experiments with the big jet again with more accurate speakers and where they can be controlled individually.

Bibliography

- [1] 4939 -1/4-inch free-field microphone, 4 hz to 100 khz, 200v polarization, <http://www.bksv.com/Products/transducers/acoustic/microphones/microphone-cartridges/4939>.
- [2] Definition of input offset voltage, <http://www.analog.com/media/en/training-seminars/tutorials/MT-037.pdf>.
- [3] Dft, http://en.wikipedia.org/wiki/Discrete_Fourier_transform.
- [4] Fast fourier transform, <http://se.mathworks.com/help/matlab/math/fast-fourier-transform-fft.html#brentpw>.
- [5] fft, <http://se.mathworks.com/help/matlab/ref/fft.html>.
- [6] The fundamentals of fft-based signal analysis and measurement in labview and labwindows/cvi, <http://www.ni.com/white-paper/4278/en/>.
- [7] Input offset voltage, http://en.wikipedia.org/wiki/Input_offset_voltage.
- [8] Moteur Ã chambre de compression tu 100, <http://www.public-adress.com/pavillons-moteurs/2289-tu100.html>.
- [9] Polyfit, <http://se.mathworks.com/help/matlab/ref/polyfit.html>.
- [10] Polynomial models, <http://se.mathworks.com/help/curvefit/polynomial.html>.
- [11] Scalar transport, <http://homepages.see.leeds.ac.uk/~amt6xw/Distance%20Learning/CFD5050TURB/node7.html>.
- [12] Strings, standing waves and harmonics, <http://newt.phys.unsw.edu.au/jw/strings.html>.
- [13] Anant Agarwal and Jeffrey H. Lang. *Foundations of Analog and Digital Electronic Circuits*.
- [14] H. H. Bruun. *Hot-wire anemometry principles and signal analysis*.

-
- [15] Mario Carbonaro. *Measurement Techniques Lecture Series*, pages 24 – 27.
- [16] Yunus A. Çengel and John M. Cimbala. *Fluid Mechanics Fundamental and Applications*.
- [17] Michael Dalton. An experimental study of a transversely forced round jet.
- [18] James R. Dawson and Nicholas A. Worth. Cinematographic oh-plif measurements of two interacting turbulent premixed flames with and without acoustic forcing.
- [19] James R. Dawson and Nicholas A. Worth. The effect of baffles on self-excited azimuthal modes in an annular combustor.
- [20] James R. Dawson and Nicholas A. Worth. Flame dynamics and unsteady heat release rate of self-excited azimuthal modes in an annular combustor.
- [21] Ken C. Everest, F. Alton; Pohlmann. *Master handbook of Acoustics*. 2009.
- [22] Françoise Baillot Florian Lespinasse. Response of a laminar premixed v-flame to a high-frequency transverse acoustic field.
- [23] Françoise Baillot Florian Lespinasse and Toufik Boushaki. Responses of v-flames placed in an hf transverse acoustic field from a velocity to pressure antinode.
- [24] H. L. Børrigter J. Buchlin M. Carbonaro G. Degrez R. Denos D. Fletcher D. Olivari M. L. Riethmüller J. Anthoine, T. Arts and A. Van den Braembussche. *Measurement techniques in fluid dynamics*.
- [25] J. Mannino J. O'Connor, C. Vanatta and T. Lieuwen. Mechanisms for flame response in a transversely forced flame.
- [26] Michael Malanowski Jacqueline O'Connor, Shweta Natarajan and Tim Lieuwen. Disturbance field characteristics of a transversely excited annular jet.
- [27] Tim Lieuwen Jacqueline O'Connor and Michael Kolb. Visualization of shear layer dynamics in a transversely excited, annular premixing nozzle. page 237, 2011.
- [28] Jonas P. Moeck Thierry Schuller Jean-Francois Bourgoignie, Daniel Durox and Sebastien Candel. Self-sustained instabilities in an annular combustor coupled by azimuthal and longitudinal acoustic modes.
- [29] Christoph Hirsch Klaas Kunze and Thomas Sattelmayer. Transfer function measurements on a swirl stabilized premix burner in an annular combustion chamber.
- [30] Erwin Kreyszig. *Advanced engineering mathematics*. 2006.

-
- [31] Maria Hasund Måløy. Characterisation of an acoustically forced transverse jet apparatus.
 - [32] Manuel Lorenz Martin Hauser and Thomas Sattelmayer. Influence of transversal acoustic excitation of the burner approach flow on the flame structure. pages 041501–1, 2011.
 - [33] Jacqueline O’Conner and Tim Lieuwen. Disturbance field characteristics of a transversely excited burner.
 - [34] L. Rayleigh. *The theory of sound*.
 - [35] D. Durox T. Schuller and S. Candel. Self-induced combustion oscillations of laminar premixed flames stabilized on annular burners.
 - [36] F. Richard Moore Thomas D. Rossing and Paul A. Wheeler. *The science of sound*. 2002.
 - [37] N. A. Worth and J. R. Dawson. Modal dynamics of self-excited azimuthal instabilities in an annular combustion chamber.
 - [38] N. A. Worth and J. R. Dawson. Self-excited circumferential instabilities in a model annular gas turbine combustor: Global flame dynamics.

Appendix A

Mass flow device

This appendix contains the actual velocities used during the experiments. The velocities are based on the SLPM from the mass flow controller.

The values was calculated using this formula:

$$SLPM \frac{[dm^3]}{[min]} = U \frac{[m]}{[s]} * r^2 \pi [m^2] * 10^3 * 60 \frac{[s]}{[min]}$$

Whanted velocity	SLPM	Actual velocity
0.5	10	0.53
5	23	4.88
10	47	9.97
15	70	14.85
20	94	19.95
25	117	24.83
30	141	29.92
35	164	34.80
40	188	39.89

Table A.1: Different velocities used during the experiments

Properties and constants

Property		Value		References
Kinematic viscosity	ν	$15,16 * 10^{-6}$	m^2s^{-1}	[16, p. 930]
Air pressure at sea level	\bar{P}	$101,1 * 10^{-3}$	Pa	Specification microphones
Speed of sound	c	343,1	ms^{-1}	[16, p.50]
Offset voltage	E_{off}	2,6	V	Measured
Temperature coefficient	α	$1,69 * 10^{-3}$	$\Omega/^{\circ}C$	Specification Wire
Resistance hotwire 20°C	R_{HWcold}	6,5-6,7	Ω	Measured
Resistance wire and cable 20°C	$R_{tot,5m}$	7,2-7,3	Ω	Measured
Gain	A	8	-	Measured

Table A.2: Different constants used during the experiments

The sound strengths in the amplifier

Amp1= 33+2

Amp11=2

Appendix B

Proving that the hotwire was reliable

Several random measurements was done with the hotwire, and then changed back to velocity based on the calibration curve. This was then plotted against the actual velocity from the mass flow controller. The line in Figure B.1, is a straight line proving that the measurements done with the hotwire was reliable. The velocities from the hotwire corresponded with the velocities from the mass flow controller.

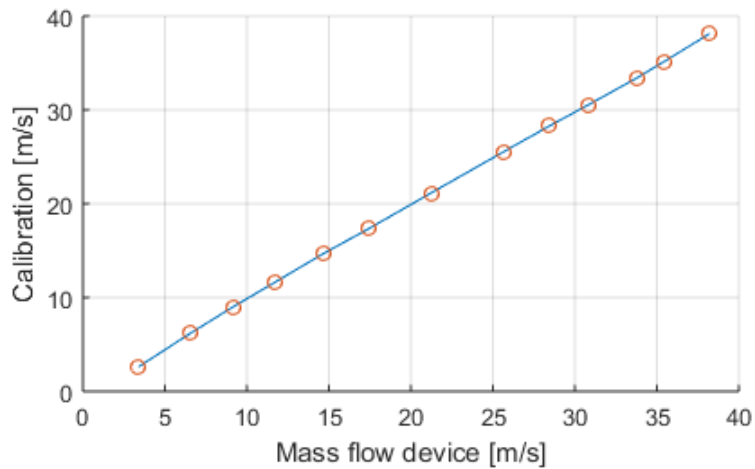


Figure B.1: Testing of the reliability of the hotwire

Appendix C

Jet profile

When trying to determine the jet profile for different velocities the measurements across the jet was done two times. Figure C.1 displays the first try. As can be seen from the figure the profiles behave correctly for 10 m s^{-1} and 30 m s^{-1} . The velocity measured divided on the velocity from the mass flow device is 1, which is correct. For 20 m s^{-1} there is 12 measured points from the left wall and out to the centre that is a little too high. This is the reason it was done a second time. These high points are an error. It could be caused by an higher mass flow stream the first measurements, meaning inaccuracy in the mass flow controller, or measurements could have been measured incorrect.

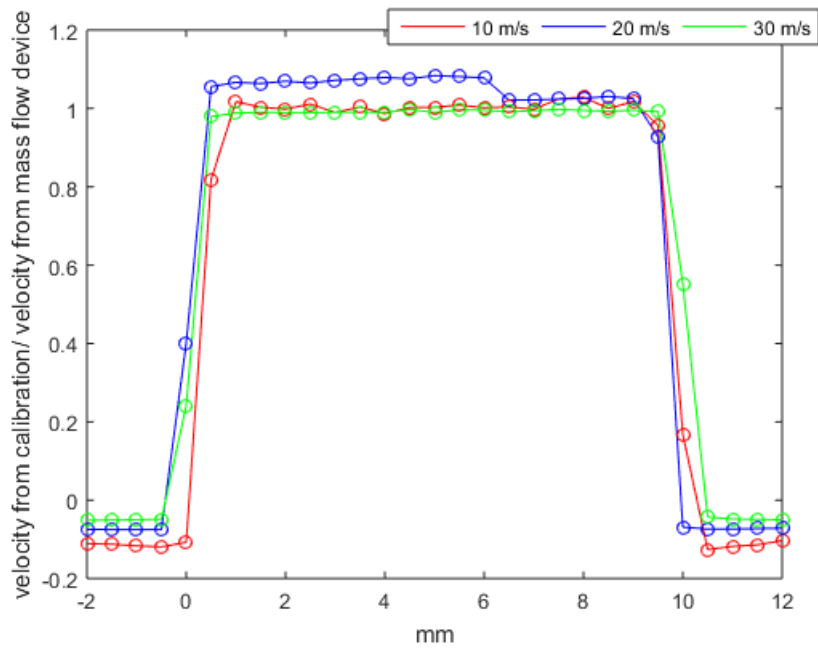


Figure C.1: Jet profile, the first try

Appendix D

Different velocities inside the small jet

Figure D.1, shows the amplitude spectrum of the pressure inside the small jet at P2. The jet have been forced while in position 1 with different velocities. The amplitudes are not correct for the forcing frequency 452 hz, since the setup of the hotwire disturbs the sound inside the box, but the only difference between these measurements are the velocity. The setup is the same for all velocities, and the forcing strength is the same amp6, meaning that the changes in the graphs is due to turbulence.

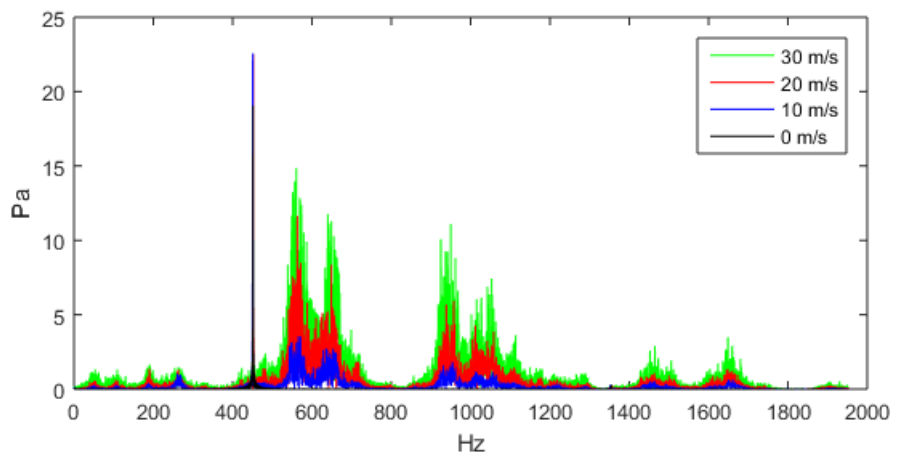


Figure D.1: Amplitude spectrum for the pressure with different velocities

The pressure measured by the microphones inside the jet at 0 m/s ($Re = 6600$) with forcing, only measures the forcing frequency 452, while at 10 m/s shows some

small turbulence disturbances. At 20 m/s ($Re = 13200$) with forcing these turbulence disturbances increase, and at 30 m/s ($Re=19800$) there are large turbulence disturbances. The same can be seen from the velocity graphs from the hotwire. The velocity amplitudes for 30 m/s can be seen in Figure D.2, and the shapes of the peaks caused by the turbulence is similar. The turbulence disturbance increases with the velocities, making it difficult to measure the peak for the forcing frequency for positions where the measured amplitude is low. Based on this the velocity of 10 m s^{-1} was chosen and used in the experiments of the small jet.

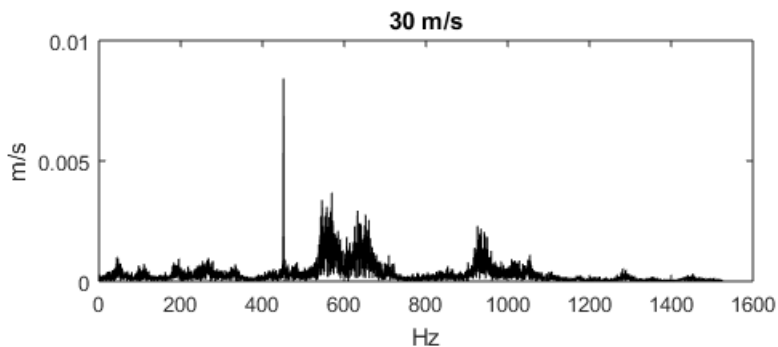


Figure D.2: Amplitude spectrum for the velocity of 30 m/s

Appendix E

When the measurements in the big jet was not as expected for $\lambda = 3$, some experimentation was done. The walls in the jet was shifted 5 mm and 10 mm and used to compare with the measurements in the original position. Notice that the microphones in the jet is not in the same position in these figures as the rest of the report, the microphones are shifted.

As can be seen from Figure E.1 compared to Figure E.2 and Figure E.3 microphones M6 and M5 have the biggest amplitude in Figure E.1 but it is the smallest in the other two figures. M1 and M2 are the strongest amplitudes in these two. This is due to the shift in the position of the node. In Figure E.1 M6 and M5 are the microphones furthest away from the node, meaning that the node is slightly closer to M3 and M8. After shifting the walls M1 and M2 are the microphones furthest away from the node. That there is some phase shift in the measured signals are very clear in all these Figures. The most interesting is were the walls have been shifted +10 mm. There is no phase difference between M1, M2, M3 and M8, and there is almost nothing between these four microphones and M4 and M7. This means that these are most likely so far away from the node that the amplitude difference between the speakers does not affect the total sum much.

The difference in the phase between M1 and M6, the microphones furthest away from each other are 95 °in the original position, 74 °at +5 mm and 50 °at +10 mm. The difference becomes smaller and smaller with the change in the position of the walls, due to the change in the position of the node.

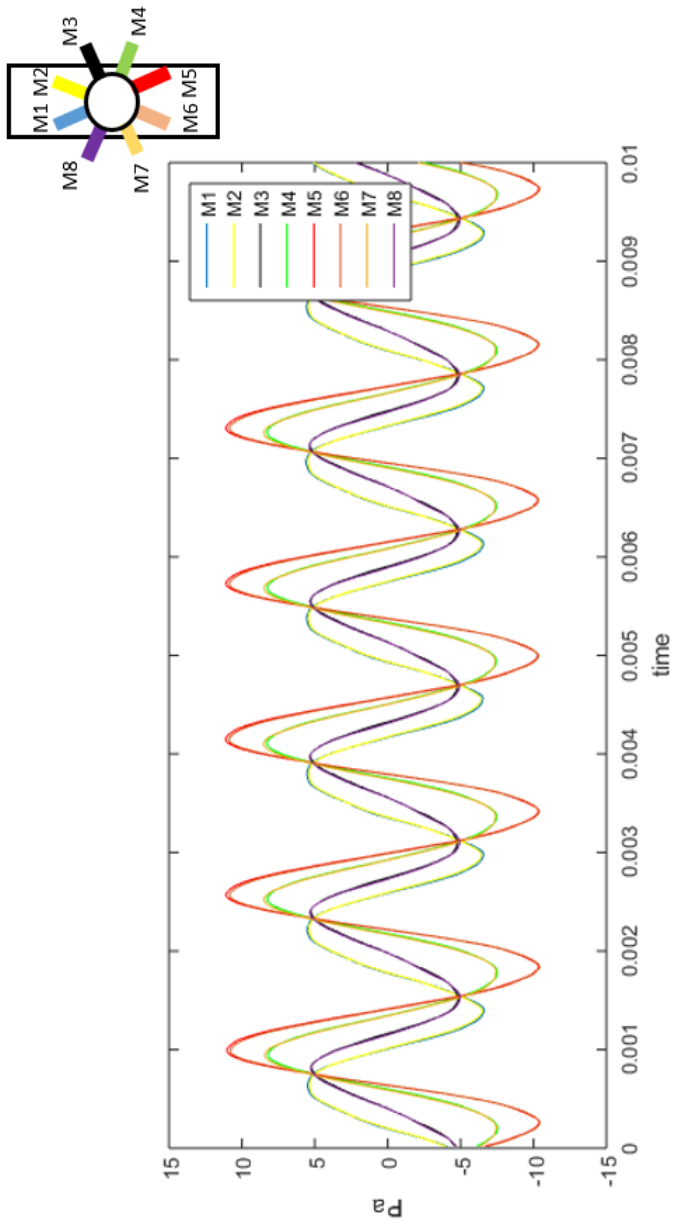


Figure E.1: Original placement

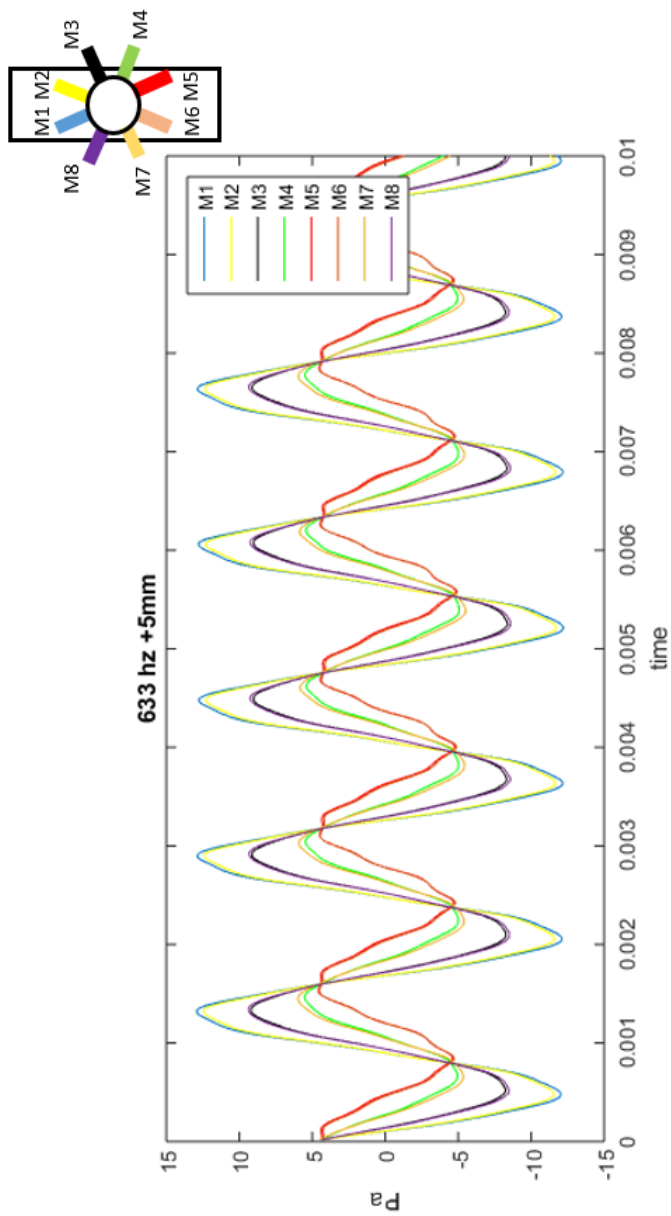


Figure E.2: + 5 mm

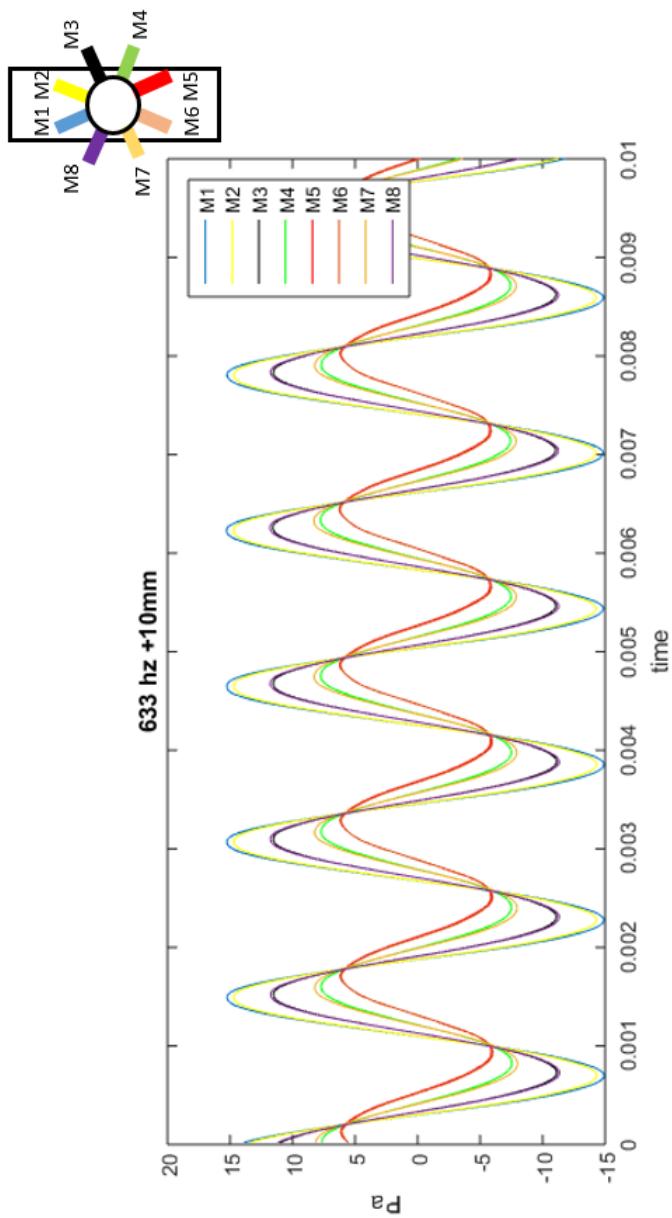


Figure E.3: + 10 mm

List of Figures

2.1	Schematics of the small jet and the box, the long side view 860 mm	5
2.2	Schematics of the box, side view 150 mm	6
2.3	Picture of the setup for the small jet	7
2.4	Picture of the hotwire above the jet, seen from the 860 mm side view	7
2.5	The dimensions of the small jet	8
2.6	The dimensions of the big jet	9
2.7	Picture of the setup of the microphones around the big jet	9
2.8	The placement of the microphones seen from the top view	10
2.9	The placement of the microphones on the wall	10
2.10	The setup for the box with the wave generator, oscilloscope, amplifier and the speakers [17]	11
2.11	Picture of one of the hotwires used.	12
2.12	The setup for the microphones [17]	13
2.13	Picture of a microphone used in the experiments [1]	14
3.1	The interaction between two waves from opposite direction, equal frequency and magnitude reinforcing each other. See the red line [12]	16
3.2	Resonance frequencies of pressure modes in a one dimensional box, 860 mm	17
3.3	Hot-wire box connected to hotwire and cDAQ	18
3.4	Hotwire CT control circuit [15, p. 27]	19
3.5	Vertical distance of a point (y_j, x_j) from a straight line $y = a + bx$	22
3.6	The square wave test response of a CT hotwire, the peak [14, p.52]	23
3.7	Sine signal with amplitude 1 and frequency of 100 hz, Fourier transformed to become an amplitude spectrum	25
3.8	Matlab coding for a Fourier transformation	26
3.9	Oversampled, critical sampled and under sampled. Figure from [36, p.485]	28
3.10	Example of 2-bit quantizer, giving 4 different values for the signal [36, p.483]	28

3.11	Example of changing back the signal taken by the 2-bit quantizer [36, p.484]	29
3.12	a) is an laminar flow while b) is an turbulent flow [11] [16, p.355]	30
4.1	A typical calibration curve	32
4.2	Calibration with and without temperature correction	33
4.3	Example of a square wave test, $\tau_w \approx 2 * 10^{-4}$ second	33
4.4	Finding the jet profiles for different velocities	34
4.5	Calibration of the microphones	35
4.6	Example of corresponding time series for the four microphones. Corresponds to 150 mV in Figure 4.5	36
4.7	Frequency Sweep of the measured amplitudes vs frequencies	37
5.1	Box 860 mm, with the different positions of the jet and the sound wave	40
5.2	Velocity time series for position 1, showing four different forcing strengths	41
5.3	Velocity time series zoomed in for Position 1, showing four different forcing strengths	41
5.4	Amplitudes for different sound strengths at Position 1	42
5.5	Amplitude spectrum of the measured velocities at Position 5 amp1	42
5.6	Time series of the pressure at Position 1	43
5.7	Time series of the pressure from P2 zoomed in, with the Fourier transformed amplitudes marked as dotted lines	44
5.8	P2 and the amplitudes of the different sine waves	44
5.9	Position 1 velocity amplitude vs pressure amplitude	45
5.10	The different positions compared to each other	46
5.11	Position 4 and 5 zoomed in	47
5.12	The different positions of the jet and the pressure amplitudes that should be measured at the different positions	48
5.13	Pressure amplitude divided on the pressure vs the position of the jet	49
5.14	Velocity amplitude divided on the velocity vs the position of the jet	49
6.1	The different amplitudes the microphones on the wall should measure when $\lambda = 3$	52
6.2	The measured amplitudes from the microphones on the wall with frequency 633 Hz	53
6.3	Amplitude spectre for M1, M5 and M11	53
6.4	The amplitudes measured by the microphone inside the jet	54
6.5	Measuring the speakers at the node, using M11	55
6.6	Simulation of sine signals travelling in the opposite direction, with different amplitudes	56
6.7	The time series from the microphones inside the jet	57

6.8	The time series from the microphones inside the jet zoomed in . . .	58
6.9	The amplitude spectrum of M7 with air	58
6.10	The amplitudes on the wall when $\lambda = 5$, compared with each other .	59
6.11	The time series of the microphones inside the jet before moving the walls	60
6.12	The time series of the microphones inside the big jet	61
6.13	The time series of the microphones of the wall	62
6.14	The time series for M11, M1 and M5	63
6.15	Amplitude spectrum for M11, M1 and M5	64
6.16	Time series for the microphones inside the jet with airflow	64
6.17	Amplitude spectrum for M1 and M3 with airflow	65
7.1	Time series $\lambda = 5$, M3 and M7, the microphone closest to each speaker	68
7.2	Two different sizes of the frequency bins same signal	69
B.1	Testing of the reliability of the hotwire	77
C.1	Jet profile, the first try	80
D.1	Amplitude spectrum for the pressure with different velocities	81
D.2	Amplitude spectrum for the velocity of 30 m/s	82
E.1	Original placement	84
E.2	+ 5 mm	85
E.3	+ 10 mm	86

List of Tables

2.1	Table of the sensitivities of the different microphones.	13
4.1	Table over the different frequencies	37
5.1	The different positions of the jet from the speaker wall	40
5.2	The velocity amplitudes and the pressure amplitudes	45
6.1	The different calculated frequencies	51
6.2	The amplitudes from the microphones inside the jet, with and without airflow	58
6.3	The amplitudes from the microphones inside the jet with and without airflow	65
A.1	Different velocities used during the experiments	75
A.2	Different constants used during the experiments	76

